Hunger- and thirst-sensing neurons modulate a neuroendocrine network to coordinate sugar and water ingestion

Authors:
Amanda J. González-Segarra[1*], Gina Pontes[1,2], Nicholas Jourjine[1,3], Alexander Del Toro[1,4], Kristin Scott[1*#]

[1]University of California, Berkeley, United States;
[2]present address: IBBEA, CONICET-UBA, Buenos Aires, Argentina;
[3]present address: Harvard University, Cambridge, United States;
[4]present address: Brown University, Rhode Island, United States

*Corresponding authors: amandagonzalez@berkeley.edu, kscott@berkeley.edu
Lead contact

ABSTRACT

Consumption of food and water is tightly regulated by the nervous system to maintain internal nutrient homeostasis. Although generally considered independently, interactions between hunger and thirst drives are important to coordinate competing needs. In *Drosophila*, four neurons called the Interoceptive Subesophageal zone Neurons (ISNs) respond to intrinsic hunger and thirst signals to oppositely regulate sucrose and water ingestion. Here, we investigate the neural circuit downstream of the ISNs to examine how ingestion is regulated based on internal needs. Utilizing the recently available fly brain connectome, we find that the ISNs synapse with a novel cell type Bilateral T-shaped neuron (BiT) that projects to neuroendocrine centers. *In vivo* neural manipulations revealed that BiT oppositely regulates sugar and water ingestion. Neuroendocrine cells downstream of ISNs include several peptide-releasing and peptide-sensing neurons, including insulin producing cells (IPC), crustacean cardioactive peptide (CCAP) neurons, and CCHamide-2 receptor isoform RA (CCHa2R-

RA) neurons. These neurons contribute differentially to ingestion of sugar and water, with IPCs and CCAP neurons oppositely regulating sugar and water ingestion, and CCHa2R-RA neurons modulating only water ingestion. Thus, the decision to consume sugar or water occurs via regulation of a broad peptidergic network that integrates internal signals of nutritional state to generate nutrient-specific ingestion.

INTRODUCTION

The survival of an organism depends on its ability to coordinate nutrient ingestion with internal nutrient abundance in order to meet its metabolic needs. The nervous system acts as an internal nutrient abundance sensor to drive ingestion in nutrient-deprived states and inhibit ingestion in nutrient-replete states to restore homeostasis (Gizowski & Bourque, 2018, Jourjine, 2017, Sternson, 2013, Qi et al., 2021, Yoshinari et al., 2021). Although generally considered independently, recent studies have demonstrated that interactions between hunger and thirst signals coordinate competing needs (Burnett et al., 2018, Cannell et al., 2016, Jourjine, Mullaney et al., 2016, Watts & Boyle, 2010, Zimmerman et al., 2016).

In mammals, regulation of hunger and thirst drives likely occurs through interactions between food and water ingestion circuits (Eiselt et al., 2021). In the arcuate nucleus of the hypothalamus, neurons that express the agouti related peptide (AgRP) and neuropeptide Y promote food ingestion while neurons that express pro-opiomelanocortin inhibit food ingestion (Aponte et al., 2011, Graham et al., 1997, Sternson, 2013). These neurons can detect circulating ghrelin, glucose, insulin, and leptin secreted from peripheral organs, in addition to receiving input from the gut

through the vagus nerve (Sternson, 2013). In the subfornical organ, neurons expressing neuronal nitric oxide synthase (nNOS) promote water ingestion while neurons expressing the vesicular GABA transporter inhibit water ingestion. These cells directly detect blood osmolality and receive input from the gut via the vagus nerve and from the mouth via the trigeminal nerve (Gizowski & Bourque, 2018, Zhang et al., 2022). Interestingly, activation of AgRP neurons decreases water ingestion and inhibition of nNOS expressing cells increases food ingestion (Burnett et al., 2016; Zimmerman et al., 2016). This suggests that hunger sensing cells promote food ingestion and inhibit water ingestion, while thirst sensing cells do the opposite (Jourjine, 2017). However, the underlying circuit mechanisms that lead to this reciprocal coordination of hunger and thirst remain unexplored.

Because of its numerically less complex nervous system, complete connectome, and abundant genetic tools, *Drosophila* is an ideal organism in which to study the coordination of hunger and thirst (Pfeiffer et al., 2008). Like mammals, *Drosophila melanogaster* selectively consumes food when hungry and water when thirsty (Dethier, 1976, Gáliková et al., 2018, Landayan et al., 2021, Lin et al., 2014, Min et al., 2016, Yapici et al., 2016). Moreover, in *Drosophila*, two pairs of neurons, the Interoceptive Subesophageal zone Neurons (ISNs), directly integrate hunger and thirst signals to oppositely regulate sugar and water ingestion (Jourjine, Mullaney et al., 2016).

The ISNs express the adipokinetic hormone receptor (AKHR), a G-protein coupled receptor which binds to the glucagon-like peptide adipokinetic hormone (AKH), a hormone released from the corpora cardiaca during starvation that signals nutrient deprivation (Orchard, 1987, Gáliková et al., 2015). AKH increases ISN activity to drive

77 sugar ingestion and reduce water ingestion. The ISNs also express the TRPV channel
78 Nanchung, which senses changes in hemolymph osmolality. High hemolymph
79 osmolality, such as that experienced during thirst, decreases ISN activity to promote
80 water ingestion and inhibit sugar ingestion (Jourjine, Mullaney et al., 2016). Thus, the
81 ISNs sense both AKH and hemolymph osmolality, arguing that they balance internal
82 osmolality fluctuations and nutrient need (Jourjine, Mullaney et al., 2016). How the ISNs
83 achieve these effects on ingestion remains unclear.

84 To investigate how the ISNs transform internal nutrient detection into changes in
85 feeding behaviors, we examined the neural network downstream of the ISNs. Using the
86 fly brain connectome, intersectional genetic approaches, *in vivo* functional imaging, and
87 behavioral assays, we identified a neural circuit downstream of the ISNs that regulates
88 sugar and water ingestion. Our work reveals that the ISNs communicate with the
89 neuroendocrine center of the fly brain and regulate the activity of a large number of
90 neurons that transmit or receive peptidergic signals of nutritive state to bidirectionally
91 regulate sugar and water ingestion.

92

93 **RESULTS**

94 **The ISNs are peptidergic neurons that release dILP3**

95 To examine how the ISNs reciprocally regulate sugar and water ingestion, we
96 aimed to identify the neural circuit downstream of the ISNs. We first sought to identify
97 which neurotransmitter the ISNs use to communicate with downstream neurons. We
98 expressed RNAi against enzymes involved in neurotransmitter synthesis, vesicular
99 transporters, and neuropeptides in the ISNs and monitored water ingestion in water

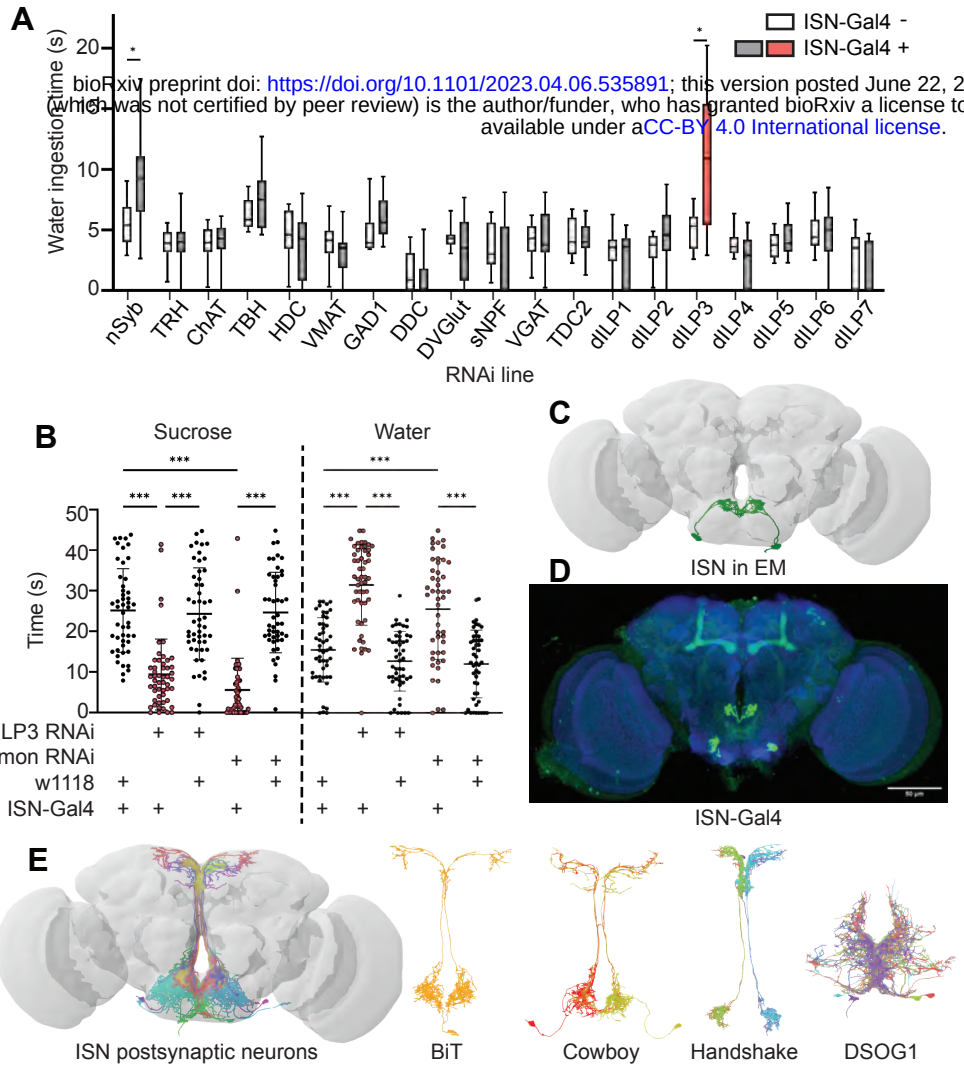

Figure 1. ISNs relay information to the Pars Intercerebralis

(A) Temporal consumption assay screen for water ingestion using RNAi targeting different neurotransmitter pathways. UAS-RNAi + or - ISN-Gal4. RNAi against: nSynaptobrevin (nSyb), tryptophan hydroxylase (TRH), choline acetyltransferase (ChAT), tyrosine beta-hydroxylase (TBH), histamine decarboxylase (HDC), vesicular monoamine transporter (VMAT), glutamic acid decarboxylase 1 (GAD1), dopa decarboxylase (DDC), Drosophila vesicular glutamate transporter (DVGlut), short neuropeptide F (sNPF), vesicular GABA transporter (VGAT), Tyrosine decarboxylase 2 (TDC2), Drosophila insulin like peptide 1 (dILP1), Drosophila insulin like peptide 2 (dILP2), Drosophila insulin like peptide 3 (dILP3), Drosophila insulin like peptide 4 (dILP4), Drosophila insulin like peptide 5 (dILP5), Drosophila insulin like peptide 6 (dILP6), Drosophila insulin like peptide 7 (dILP7). Represented are the mean, and the 10-90 percentile; data was analyzed using Kruskal-Wallis test, followed by multiple comparisons against the RNAi control; p-values were adjusted using False Discovery Rate. n=8-39 animals/genotype except nSyb positive control (70-72). (B) Temporal consumption assay for 1M sucrose or water using RNAi targeting dILP3 or amontillado in ISNs. Sucrose assay: Kruskal-Wallis test followed by Dunn's multiple comparison tests against ISN control and respective RNAi control. Water assay: ANOVA, Šídák's multiple comparison test to ISN control and respective RNAi control. n=48-52 animals/genotype. (C) ISNs reconstruction from FAFB volume. (D) Light microscopy image of ISN-Gal4 registered to JFRC2010. (E) ISN postsynaptic neurons based on synapse predictions using FAFB volume (Zheng et al. 2018) and connectome annotation versioning engine (CAVE, Buhmann et al. 2021, Heinrich et al. 2018). Left: 10 postsynaptic neurons, right: postsynaptic neurons BiT, Cowboy, Handshake and DSOG1. *p<0.05, ***p<0.001

deprived flies (Figure 1A). As decreasing activity of the ISNs increases water ingestion (Jourjine, Mullaney et al., 2016), we anticipated that an RNAi against the ISN neurotransmitter would decrease neurotransmission and increase water ingestion. Interestingly, in an RNAi screen of 18 common neurotransmitters and neuropeptides, only suppression of *Drosophila* insulin-like peptide 3 (dILP3) in the ISNs altered water ingestion (Figure 1A).

To confirm that dILP3 functions in the ISNs and to test whether it is involved in the reciprocal regulation of water and sugar ingestion, we expressed RNAi against dILP3 in the ISNs and measured sugar or water ingestion in water sated or thirsty flies respectively (Figure 1B). As an additional approach to reduce dILP3, we expressed an RNAi against a neuropeptide processing protease, *amontillado* (Siekhaus & Fuller, 1999), in the ISNs and tested sugar and water ingestion. We found that knockdown of either dILP3 or *amontillado* in the ISNs caused both a decrease in sugar ingestion and an increase in water ingestion (Figure 1B). This is the same phenotype that was previously reported in the ISNs upon loss of neurotransmission (Jourjine, Mullaney et al., 2016). These data argue that the ISNs are peptidergic neurons that release dILP3 and that one function of dILP3 is to promote sugar ingestion and inhibit water ingestion.

The ISNs synapse onto neurons that arborize in neuroendocrine and feeding centers

Drosophila has one insulin-like receptor (dInR), a tyrosine kinase type receptor homologous to the human insulin receptor, which binds dILP3 and six of the additional *Drosophila* insulin-like peptides (Brogiolo et al., 2001, Claeys et al., 2002, Clancy et al.,

2001, Fernandez, et al., 1995, Grönke et al., 2010, Nässel & Broeck, 2016, Tatar et al., 2001). In adult flies, insulin signaling has been shown to regulate an array of physiological processes including metabolism, feeding, reproduction, and lifespan (Badisco et al., 2013, Biglou et al., 2021, Clancy et al., 2001, Nässel et al., 2013, Ohhara et al., 2018). Since dInR is ubiquitous and involved in many different processes (Chen et al., 1996, Garofalo, 2002, Veenstra et al., 2008), we could not leverage neurotransmitter receptor identity for postsynaptic neuron identification. We instead used the *trans*-Tango system (Talay et al., 2017), a genetic trans-synaptic tracer, to label neurons postsynaptic to the ISNs (Supp 1A). We expressed the *trans*-Tango ligand in the ISNs and its receptor panneurally. Binding of the ligand to its receptor induces GFP expression in the receptor-expressing cells and labels potential synaptic partners (Talay et al., 2017). *trans*-Tango labeling revealed numerous ISN postsynaptic arborizations in the subesophageal zone (SEZ), a brain region associated with taste processing and feeding circuits (Gordon & Scott, 2009, Scott et al., 2001, Wang et al., 2004), and along the median bundle to the superior medial protocerebrum (SMP), a neuroendocrine center (Hartenstein, 2006, Nässel & Zandawala, 2020) (Supp 1A). However, as many ISN candidate postsynaptic neurons were labeled, the morphology of individual neurons was unclear.

To comprehensively examine the postsynaptic partners of the ISNs, we employed the Full Adult Fly Brain (FAFB) volume, a whole-brain electron microscopy volume that provides synaptic resolution of all neurons in the fly brain (Zheng, Lauritzen et al., 2018). We manually reconstructed the ISNs using CATMAID (Li et al., 2019, Saalfeld et al., 2009) by tracing neuronal arbors from the pharyngeal nerve with large

cell bodies in the SEZ. Due to the ISNs' unique morphology, with large cell bodies near the pharyngeal nerve and dense neurites in the flange that cross the midline, we used visual morphological comparison of the reconstructed ISNs in the FAFB volume (Figure 1C) and light microscopy images of *ISN-Gal4* (Figure 1D) to identify the ISNs. Once we had reconstructed the ISNs, we labeled presynaptic sites in the ISNs and postsynaptic sites in other neurons based on known synapse active zone structure (Zhai & Bellen, 2004). We then reconstructed neurons that were postsynaptic to the ISNs.

Soon after we had reconstructed the four ISNs and several postsynaptic neurons in CATMAID, the FlyWire whole brain connectome of more than 80,000 reconstructed EM neurons became available (Dorkenwald et al., 2022, flywire.ai). Since FlyWire uses the FAFB volume, we used the coordinates of the ISNs we traced in CATMAID to locate them in FlyWire. Additionally, we compared a pointcloud generated from a registered light microscopy image of *ISN-Gal4* (Figure 1D) to the reconstructed ISNs in the FAFB volume (Figure 1C) to further confirm ISN identity. We identified neurons downstream of the ISNs (Fig 1E). We found that the ISNs have 104 predicted postsynaptic partners with 5 or more synapses, comprising 9 morphological cell types (Supplementary Table 1, Supp 1C-K). These include known cell types (Cowboy, DSOG1, FLAa2, FLAa3/Lgr3 and the ISNs; Lee et al., 2020, Pool et al., 2014, Sterne et al., 2021, Yu et al., 2013) as well as many uncharacterized cell types. The ISN predicted postsynaptic partners include projection neurons that project along the median bundle to the SMP (64 cells), local SEZ neurons (18 cells), ascending neurons with projections coming through the neck connective (10 cells), descending neurons with projections leaving through the neck connective (8 cells), and the ISNs themselves (4 cells). This connectivity is

consistent with the connectivity determined by *trans*-Tango (Supp 1A). Overall, the ISN synaptic connectivity suggests that the hunger and thirst signals sensed by the ISNs are conveyed to a broad network, with the potential to coordinate feeding behaviors (SEZ neurons), nutrient status (SMP neuroendocrine centers), and movement or digestion (ascending and descending neurons). We note that as neuropeptides may diffuse over long distances (van den Pol, 2012), ISN dILP3 release may also influence activity of additional neurons that are not synaptically connected to the ISNs.

The ISN postsynaptic neuron BiT reciprocally regulates sugar and water ingestion

As the majority of the ISN predicted postsynaptic partners project to the SMP, we examined whether ISN communication to this region regulates neuroendocrine cells and/or influences feeding behavior. As a first step, we focused on an uncharacterized neuron that receives the most synaptic input from the ISN per single cell. We named this neuron Bilateral T-shaped neuron (BiT). BiT has its cell body in the SEZ and bilateral projections in the flange and SMP. It receives 7.4% of ISN synaptic output (301/4050 synapses) (Supp 1B and Supplementary Table 1). In turn, the ISNs are the main synaptic input to BiT, comprising 17% of BiT's synaptic input (301/1763 synapses). We generated a split-Gal4 line that labels BiT to study its function (Fig 2B). We screened over 20 AD-DBD combinations and found that *VT002073-Gal4.AD* and *VT040568-Gal4.DBD* specifically labeled BiT. We confirmed this by comparing a pointcloud generated from a registered light microscopy image of *BiT split-Gal4* (Fig 2B) with the reconstructed BiT in the FAFB volume (Fig 2A).

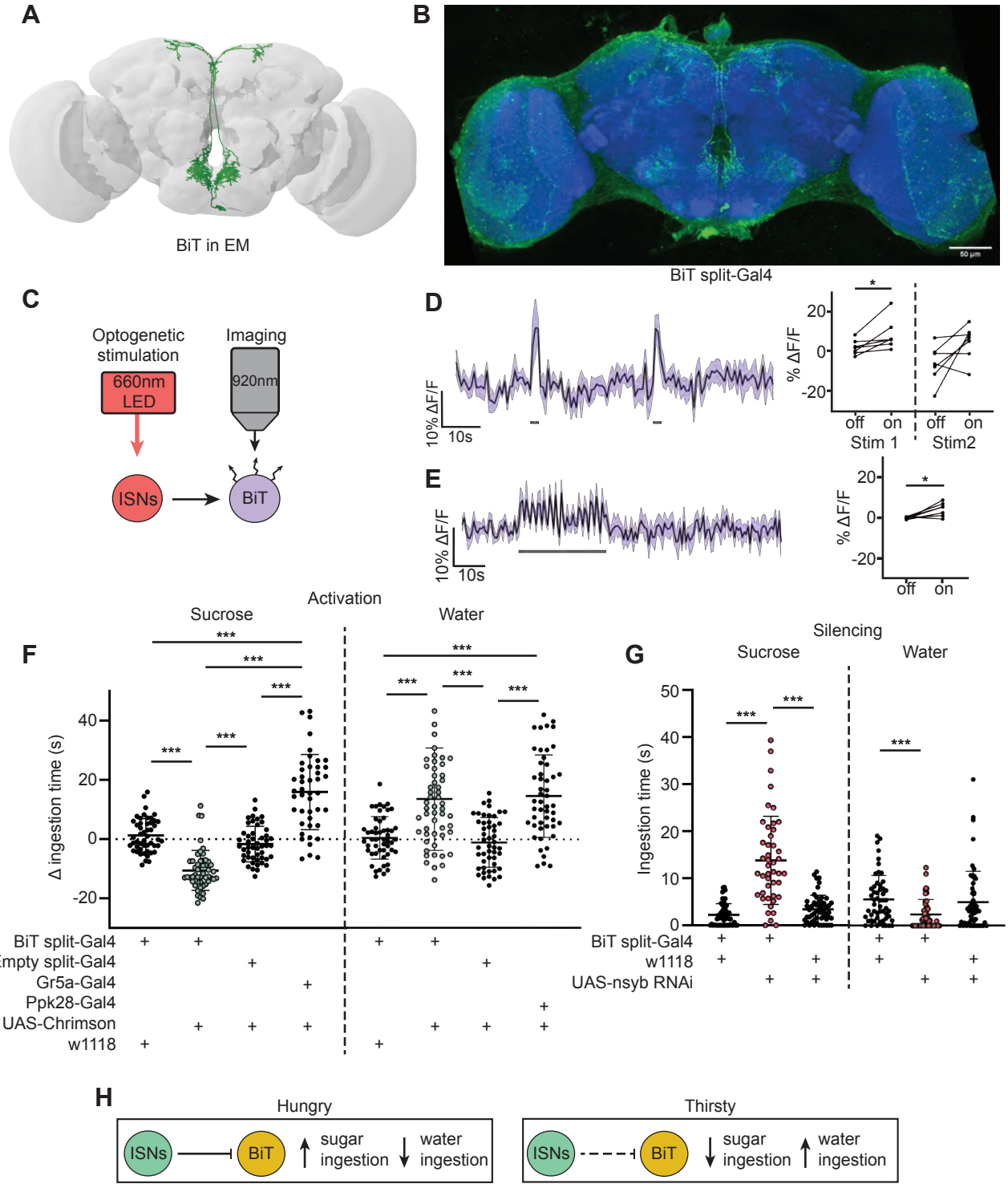

Figure 2. ISNs inhibit BiT, which oppositely regulates sugar and water ingestion
(A) BiT neuron reconstruction from FAFB dataset. (B) Light microscopy image of BiT split-Gal4. (C) Experimental setup for in vivo voltage imaging. We expressed the light sensitive ion channel Chrimson in the ISNs and optogenetically stimulated them with 660nm LED. We expressed the voltage sensor ArcLight in BiT and imaged it with a 2 photon microscope. (D) ArcLight response of BiT soma to 2s optogenetic stimulation of the ISNs or (E) 30s optogenetic stimulation of the ISNs. Left: Scatter plot shows mean +/- SEM of all flies imaged, gray bars represent LED stimulation. Right: Quantification of mean fluorescence intensity before stim (off) and during stim (on), each dot represents one fly. Paired Wilcoxon and paired t-test (Stim 2, p=0.07). n=7 flies. (F) Temporal consumption assay for 1M sucrose or water during acute optogenetic activation of BiT with Chrimson. Ingestion time of females exposed to light normalized to dark controls of indicated genotype. Sucrose: Kruskal-Wallis test with Dunn's multiple comparison test. Water: One-way ANOVA with Holm-Šídák multiple comparison test. n=44-54 animals/genotype.(G) Temporal consumption assay for 1M sucrose or water using RNAi targeting nSyb in BiT. Kruskal-Wallis with Dunn's multiple comparison test. n=45-57 animals/genotype. (H) Neural model for BiT coordination of sucrose and water intake. Dashed lines indicate inactive synapses. *p<0.05, ***p<0.001

To test whether the ISNs are functionally connected to BiT, we conducted *in vivo* functional imaging experiments in which we activated the ISNs while simultaneously monitoring BiT's neural activity. We expressed the light activated cation channel Chrimson in the ISNs and the voltage sensor ArcLight in BiT (Fig 2C) (Jin et al., 2012, Klapoetke et al., 2014). In one experiment, we applied two consecutive 2s stimulations (Fig 2D) to test whether the response was reproducible. In another experiment, we applied a longer 30s stimulation (Fig 2E) to ensure we captured the full response to ISN stimulation since dILPs can act over longer time scales (Sudhakar et al., 2020). In both experiments, we found that stimulating the ISNs increased ArcLight fluorescence in BiT, demonstrating that BiT became hyperpolarized (Fig 2D-E). Oscillation in BiT's response during the 30s stimulation (Fig 2E) is due to oscillations in the LED stimulation paradigm. Thus, increased activity in the ISNs inhibits BiT.

Next, we tested whether BiT modulates sugar or water ingestion. We measured total ingestion time of sugar or water while activating or inhibiting BiT. We found that acute optogenetic activation of BiT decreased sugar ingestion and increased water ingestion (Fig 2F). Moreover, reducing synaptic transmission in BiT using nSynaptobrevin (nSyb) RNAi caused increased sugar ingestion and decreased water ingestion (Fig 2G). These data demonstrate that BiT is both necessary and sufficient to regulate sugar and water ingestion. Furthermore, we find that the activation and silencing phenotypes for BiT are opposite to the ISN phenotypes, consistent with our calcium imaging studies that the ISNs inhibit BiT. These findings reveal that the coordination of sugar and water ingestion is maintained downstream of the ISNs.

These studies demonstrate that BiT activity reciprocally regulates sugar and water ingestion, similar to the ISNs. Hunger signals (i.e. adipokinetic hormone) activate the ISNs, causing the ISNs to inhibit BiT, which in turn increases sugar ingestion. On the other hand, thirst signals (i.e. high hemolymph osmolality) inhibit the ISNs, releasing ISN inhibition onto BiT, causing an increase in water ingestion (Fig 2H). Strikingly, although BiT is only one ISN downstream neuron, its activity increases and decreases are sufficient to coordinate both sugar and water ingestion, suggesting that it is a critical node in the ISN network.

BiT downstream partners include neuroendocrine cells that convey nutritional status

To examine how BiT coordinates sugar and water ingestion, we investigated the neural circuit downstream of BiT using the FlyWire connectome (Fig 3). The FAFB connectivity revealed that BiT has 93 predicted postsynaptic partners. Unlike the ISNs' downstream partners, which only innervate the SMP and SEZ, BiT postsynaptic partners reach more brain regions including the superior lateral protocerebrum (SLP), fan shaped body (FB), lobula, SMP, and SEZ. This suggests that the hunger and thirst signals detected by the ISNs are conveyed by BiT to widely regulate brain activity.

Many of the BiT predicted postsynaptic partners arborize in both the SEZ and SMP, suggesting that they might coordinate nutritional status and feeding. Several BiT targets transmit or receive peptidergic signals of nutrient state. For example, BiT postsynaptic partners include insulin producing cells (IPCs), FLAa3/Lgr3 neurons, and neurons labeled by the *CCHa2R-RA-Gal4* line (Deng et al., 2019) (Fig 3,

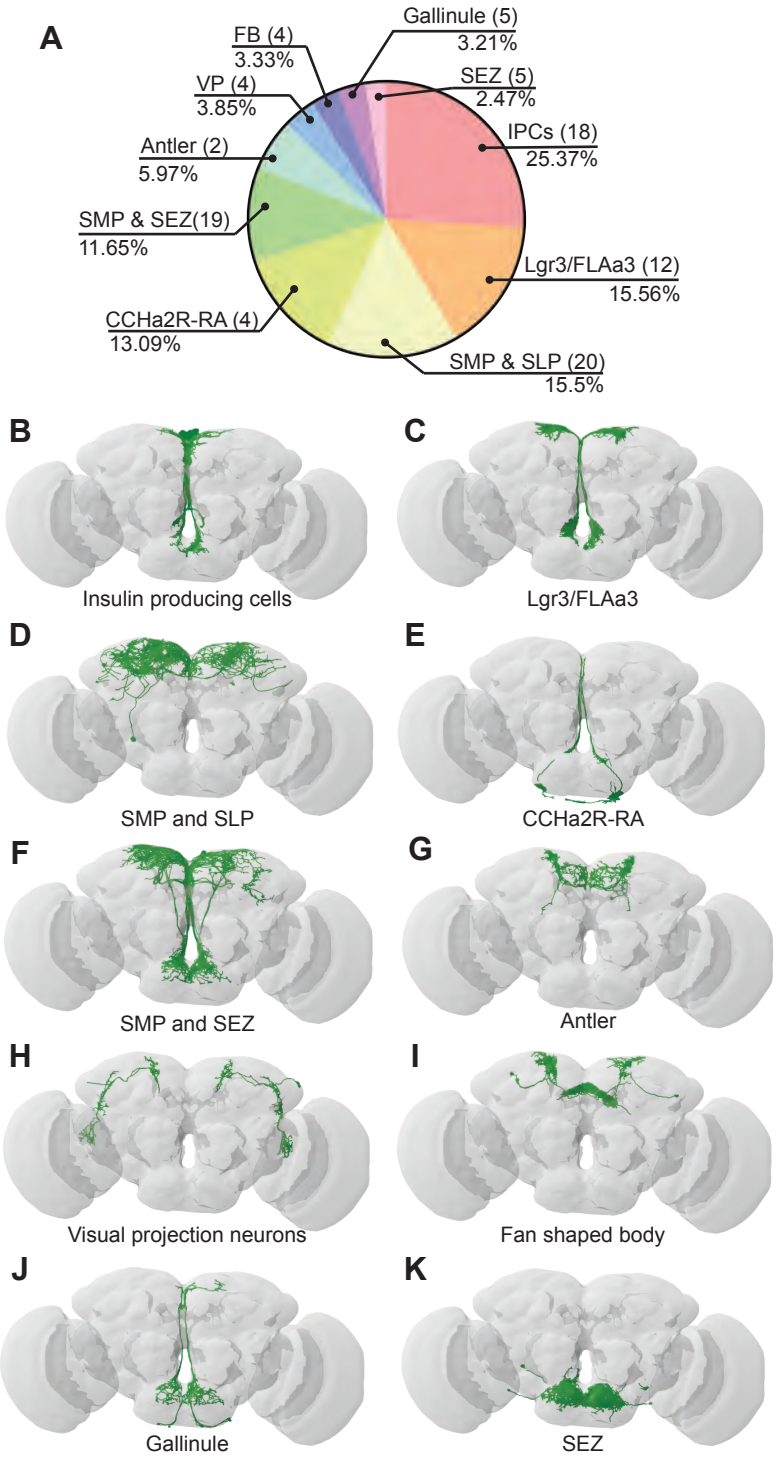

Figure 3. BiT postsynaptic neurons include neuroendocrine cells

(A) Distribution of synaptic output from BiT divided by cell class or brain region. Total of 1742 synapses from BiT and 93 postsynaptic partners. IPCs (18 neurons) receive 25.37% of all BiT output, Lgr3/FLAa3 (12 neurons) 15.56%, SMP and SLP (20 neurons) 15.5%, CCHa2R-RA (4 neurons) 13.09%, SMP and SEZ (19 neurons) 11.65%, Antler (2 neurons) 5.97%, visual projections (4 neurons) 3.85%, fan shaped body (4 neurons) 3.33%, Gallinule (5 neurons) 3.21%, SEZ (5 neurons) 2.47%. Only post-synaptic partners with 5 or more synapses were considered for this analysis. Reconstruction of IPCs (B), Lgr3/FLAa3 neurons (C), neurons innervating the SMP and SLP (D), CCHa2R-RA neurons (E), neurons innervating the SMP and SEZ (F), Antler neurons (G),visual projection neurons (H), neurons innervating the fan shaped body (I), Gallinule neurons (J), and neurons innervating the SEZ (K).

Supplementary Table 2). IPCs are a well-studied cell type that release dILP2, dILP3 and dILP5, regulate glucose uptake, and influence many physiological processes including feeding (Nässel et al., 2013, Ohhara et al., 2018). FLAa3/Lgr3 neurons detect dILP8 and influence sugar ingestion (Meissner et al., 2016, Yeom et al., 2021, Yu et al., 2013). CCHa2 and its receptor CCHa2R have been shown to participate in feeding regulation and regulate insulin signaling, although the function of CCHa2R-RA neurons has not been examined (Deng et al., 2019, Ida et al., 2012, Ren et al., 2015, Sano et al., 2014, Shahid et al., 2021). Thus, BiT is predicted to synapse onto many neuroendocrine neurons, possibly enabling integration of the hunger and thirst signals sensed by ISNs with diverse nutrient state signals.

IPCs regulate sugar and water ingestion

The IPCs integrate multiple signals of nutrient status and regulate feeding and metabolism (Nässel & Zandawala, 2020). We found that the ISNs are connected to the IPCs via BiT. BiT is the main synaptic input into IPCs, making up 25% of the IPCs' synaptic input (442/1735) and IPCs receive 25% of BiT's synaptic output (442/1742) (Fig 3, Table 2). We tested whether BiT is functionally connected to the IPCs by optogenetically stimulating BiT and monitoring activity in IPCs using the calcium sensor GCaMP6s (Chen et al., 2013). We found that BiT inhibits IPCs (Supp 3A-B), consistent with neurotransmitter predictions (Eckstein et al., 2020) that BiT uses glutamate, which can act as an inhibitory neurotransmitter in *Drosophila* (Liu et al., 2013).

To test whether IPCs modulate ingestion of sucrose or water under conditions that reveal ISN behavioral phenotypes, we measured ingestion time of sucrose or water

while acutely activating the IPCs. We found that acute activation of IPCs increased sucrose ingestion and decreased water ingestion (Supp 3E). These results are consistent with one study (Sudhakar et al., 2020) but differ from other studies showing that acute IPC activation limits ingestion of sucrose or food (Nässel et al., 2015, Wang et al., 2020). IPCs integrate many signals and release multiple peptides (Sano et al., 2015, Söderberg et al., 2012, Ohhara et al., 2017, Wang et al., 2020), suggesting that differences in these behavioral results may, in part, stem from differences in the current nutritional state sensed by the IPCs. While further experiments are needed to elucidate how IPCs coordinate nutrient state and ingestion under different conditions, our results show that BiT regulates IPC activity and that IPC activity coordinates both sugar and water ingestion.

CCHa2R-RA neurons regulate water ingestion downstream of BiT

A number of studies indicate that CCHa2 and its receptor CCHa2R promote food intake and appetite in various insects, including blowflies (Ida et al., 2012), aphids (Shahid et al., 2021) and *Drosophila* (Ren et al., 2015). BiT synapses with CCHa2R-RA neurons, four neurons with cell bodies in the SEZ and arbors in the flange and pars intercerebralis (PI) (Fig 4B). BiT is the dominant input onto CCHa2R-RA neurons, comprising 94% of CCHa2R-RA presynaptic sites (171/181 synapses). CCHa2R-RA neurons receive the most output from BiT per single cell comprising 13% of BiT's output (228/1742 synapses). To investigate whether BiT's synaptic input to CCHa2R-RA neurons regulates ingestion, we examined the functional connectivity between BiT and

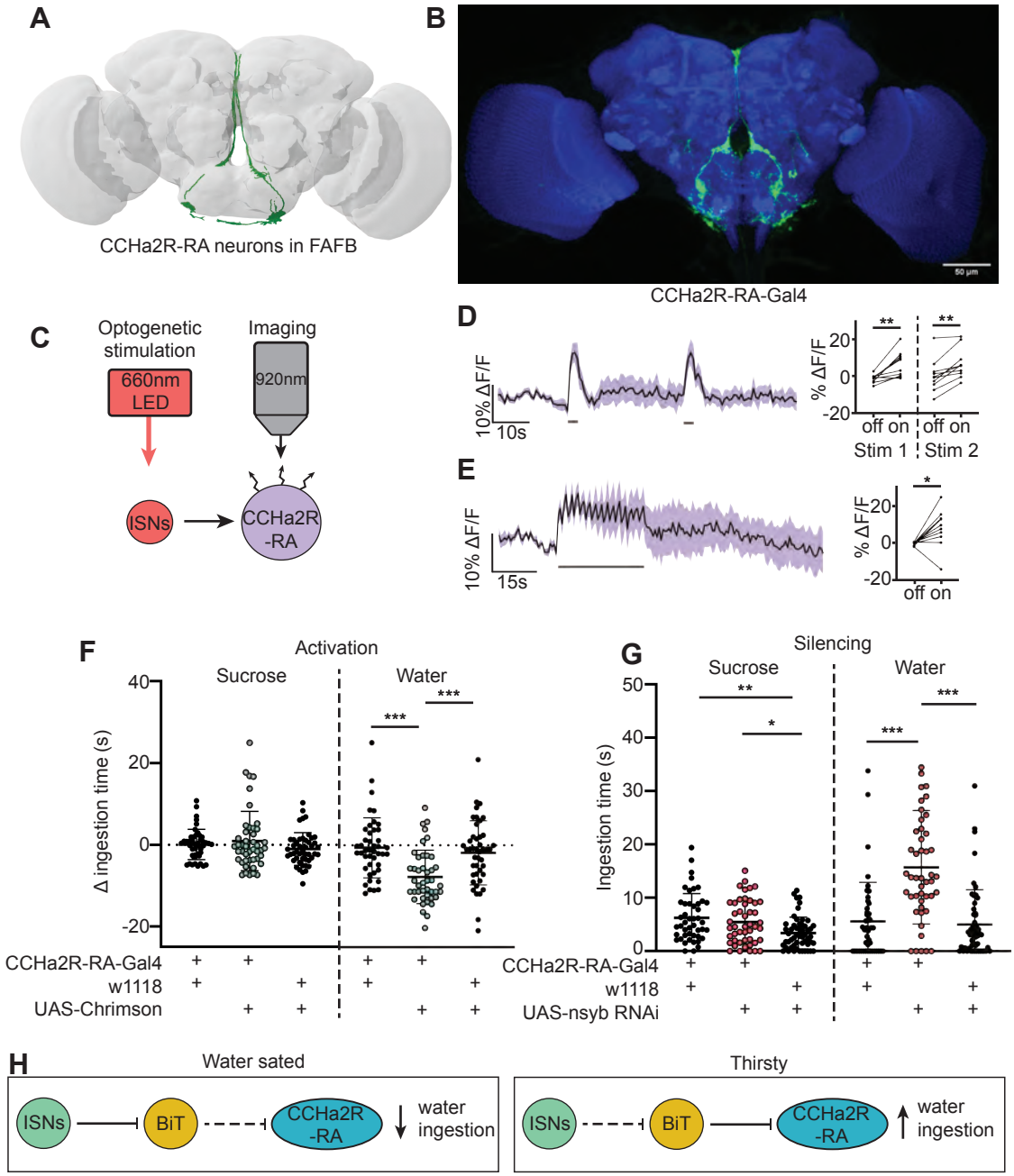

Figure 4. CCHa2R-RA neurons regulate water but not sugar ingestion and are likely inhibited by BiT
(A) CCHa2R-RA neurons reconstruction from FAFB dataset. (B) Light microscopy image of CCHa2R-RA-Gal4. (C) Experimental setup for in vivo calcium imaging. We expressed the light sensitive ion channel Chrimson in the ISNs and optogenetically stimulated them with 660nm LED. We expressed the calcium sensor GCaMP in the CCHa2R-RA neurons and imaged them with a 2 photon microscope. (D) Calcium responses of CCHa2R-RA neurites in SEZ to 2s optogenetic stimulation of the ISNs or (E) 30s optogenetic stimulation of the ISNs. Left: Scatter plot shows mean +/- SEM of all flies imaged, gray bars represent LED stimulation. Right: Quantification of mean fluorescence intensity before stim (off) and during stim (on), each dot represents one fly. Paired t-test and paired Wilcoxon test. n=10 flies. (F) Temporal consumption assay for 1M sucrose or water during acute optogenetic activation of CCHa2R-RA neurons with Chrimson. Ingestion time of females exposed to light normalized to dark controls of indicated genotype. Sucrose: Kruskal-Wallis with Dunn's multiple comparison test. Water: One-way ANOVA with Holm-Šídák multiple comparison test. n=42-47 animals/genotype. (G) Temporal consumption assay for 1M sucrose or water using RNAi targeting nSyb in CCHa2R-RA neurons. Kruskal-Wallis with Dunn's multiple comparison test. n=45-54 animals/genotype. (H) Neural model for CCHa2R-RA regulation of water intake. Dashed lines indicate inactive synapses. *p<0.05, **p<0.01, ***p<0.001

CCHa2R-RA neurons and the behavioral phenotypes associated with CCHa2R-RA neurons.

We monitored activity in CCHa2R-RA neurons with the calcium indicator GCaMP6s upon optogenetic stimulation of BiT; however, we did not observe a response in CCHa2R-RA neurons (Supp 4D-E). As BiT likely inhibits CCHa2R-RA neurons, it is possible that we were unable to detect an inhibitory response in CCHa2R-RA neurons using a calcium sensor. We therefore monitored activity of CCHa2R-RA neurons upon optogenetic stimulation of the ISNs, as the ISNs should activate CCHa2R-RA neurons given that the ISNs inhibit BiT (Fig 4C). Indeed, we found that CCHa2R-RA neurons showed robust calcium responses upon ISN stimulation (Fig 4D-E), demonstrating that these neurons are functionally connected to the ISNs, likely via BiT inhibition.

To test if CCHa2R-RA neurons regulate sugar or water ingestion, we manipulated activity in these neurons and measured ingestion of sugar or water. We found that activation of CCHa2R-RA neurons decreased water ingestion but did not change sugar ingestion (Fig 4F). Moreover, inhibiting neurotransmission in CCHa2R-RA neurons increased water ingestion (Fig 4G), but did not change sucrose ingestion relative to *CCHa2R-RA-Gal4* controls. These behavioral experiments demonstrate that peptide-sensing neurons downstream of the ISNs regulate water ingestion. The finding that CCHa2-RA neurons recapitulate the water ingestion phenotypes of the ISNs but not sugar ingestion phenotypes suggests that the ISNs activate different arrays of peptidergic neurons that contribute differentially to ingestion of specific nutrients.

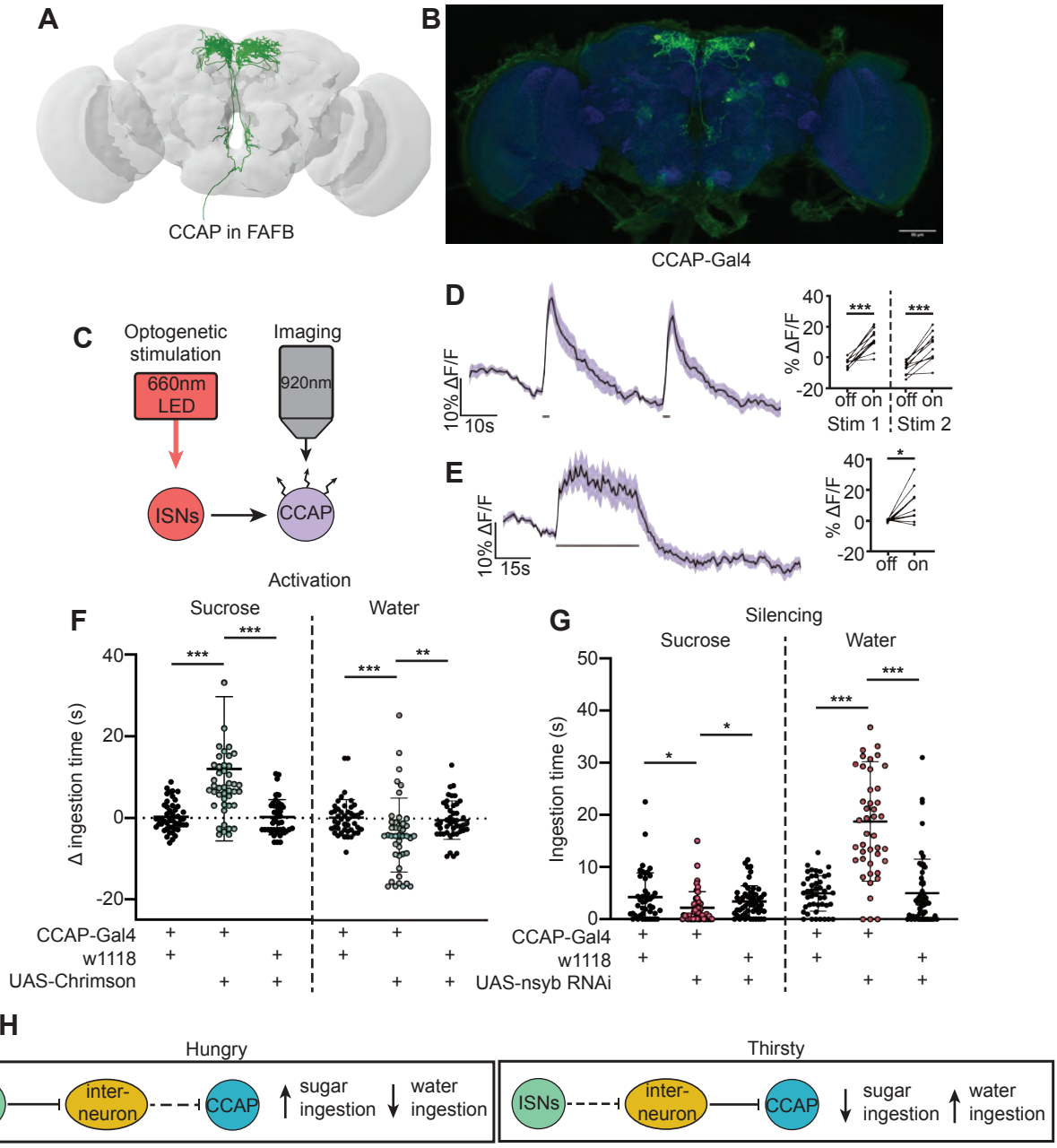

Figure 5. CCAP neurons are downstream of the ISNs and oppositely regulate sugar and water ingestion
(A) CCAP neurons reconstruction from FAFB dataset. (B) Light microscopy image of CCAP-Gal4. (C) Experimental setup for in vivo calcium imaging. We expressed the light sensitive ion channel Chrimson in the ISNs and optogenetically stimulated them with 660nm LED. We expressed the calcium sensor GCaMP in the CCAP neurons and imaged them with a 2 photon microscope. (D) Calcium response of CCAP neurites to 2s optogenetic stimulation of the ISNs or (E) 30s optogenetic stimulation of the ISNs. Left: Scatter plot shows mean +/- SEM of all flies imaged, gray bars represent LED stimulation. Right: Quantification of mean fluorescence intensity before stim (off) and during stim (on), each dot represents one fly. Paired t-test. n=10 flies. (F) Temporal consumption assay for 1M sucrose or water during acute optogenetic activation of CCAP neurons with Chrimson. Ingestion time of females exposed to light normalized to dark controls of indicated genotype. Sucrose: Kruskal-Wallis with Dunn's multiple comparison test, Water: One-way ANOVA with Holm-Šídák multiple comparison test. n=42-48 animals/genotype. (G) Temporal consumption assay for 1M sucrose or water using RNAi targeting nSyb in CCAP neurons. Kruskal-Wallis with Dunn's multiple comparison test. n=45-54 animals/genotype. (H) Neural model for CCAP coordination of sugar and water intake. Dashed lines indicate inactive synapses. *p<0.05, **p<0.01, ***p<0.001

CCAP neurons are downstream of the ISNs and reciprocally regulate sugar and water ingestion

In a separate effort to find neurons that are postsynaptic to the ISNs, we tested whether neurons that had previously been implicated in ingestion were functionally connected to the ISNs. We conducted pilot *in vivo* functional imaging experiments monitoring the activity of candidate neurons with GCaMP7b while optogenetically stimulating the ISNs. We found one set of peptidergic neurons, the crustacean cardioactive peptide (CCAP) neurons, that were activated upon ISN optogenetic stimulation (Fig 5D-E).

CCAP neurons have been shown to regulate feeding behavior in adult *Drosophila* as loss of CCAP in these neurons reduced sucrose ingestion (Williams et al., 2020). To directly test if CCAP neural activity modulates sugar or water ingestion, we acutely manipulated the activity of CCAP neurons and measured ingestion of sugar or water. We found that activation of CCAP decreased water ingestion and increased sugar ingestion (Fig 5F). To test whether CCAP neurons are necessary for sugar and water ingestion, we reduced CCAP neurotransmission with nSyb RNAi, and measured ingestion of sugar or water. We found that silencing CCAP neurons decreased sugar ingestion and increased water ingestion (Fig 5G), demonstrating that CCAP neurons reciprocally regulate sugar and water ingestion, similar to the ISNs.

Although CCAP neurons are functionally connected to the ISNs, their synaptic connectivity is indirect. We identified the CCAP neurons in the FAFB volume (Fig 5A) and found weak connections between CCAP neurons and ISN synaptic partners: Cowboy (5 synapses), VESa1 (22 synapses), and a novel neuron we named Bilateral T-

shaped neuron 2, based on its anatomical similarities to BiT (37 synapses). In addition, the ISN third-order neuron CCHa2R-RA neurons provide 26 synapses onto CCAP neurons (Supplementary Table 3). This connectivity suggests that CCAP neurons are part of the broad network that receives ISN input (Fig 5H). Moreover, the reciprocal regulation of sugar and water ingestion by CCAP neurons argues that multiple peptidergic neurons downstream of the ISNs cooperate to coordinate ingestion of sugar versus water based on specific need.

DISCUSSION

In this study, we report that the ISNs communicate hunger and thirst states to a complex neural network that reaches several brain regions to regulate sugar and water ingestion (Fig 6). The ISNs synapse with neurons that project to higher brain neuroendocrine centers, including BiT, a novel neuron that reciprocally regulates sugar and water ingestion. Several peptide-releasing and peptide-sensing neurons known to regulate feeding behavior also receive ISN signals, providing the capacity to integrate hunger and thirst signals with many internal signals of nutritional need. These peptidergic neurons, connected to the ISNs via interneurons, contribute differentially to ingestion of sugar and water, with IPC and CCAP neurons reciprocally regulating sugar and water ingestion and CCHa2R-RA neurons modulating water ingestion. Thus, our work argues that the coordinated regulation of a peptidergic network weighs nutrient needs to generate nutrient-specific ingestion.

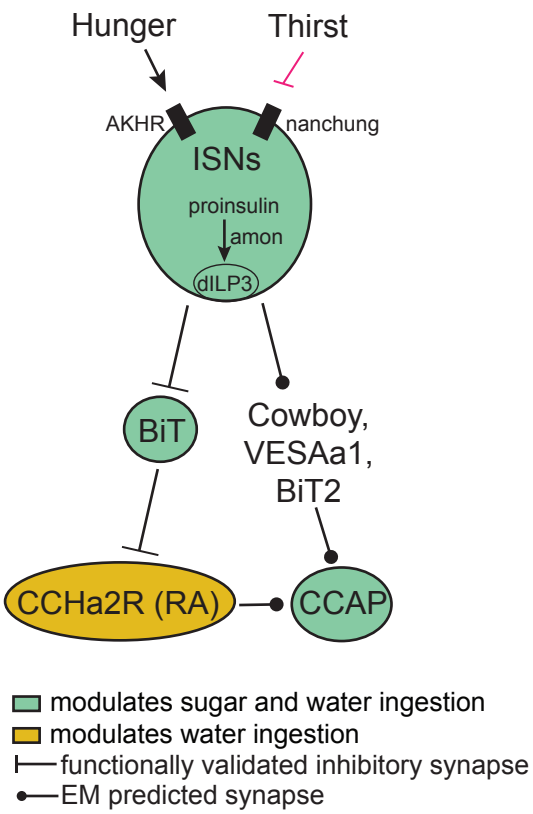

Figure 6: ISN regulation of sugar and water ingestion model
Hunger signals activate the ISN while thirst signals inhibit the ISNs. ISNs use dILP3 as a neurotransmitter and require amontillado (amon) for neuropeptide processing. ISN activity inhibits BiT, which in turn inhibits CCHa2R-RA neurons. CCAP neurons are downstream of the ISNs, connected via Cowboy, VESAa1, BiT2 and CCHa2R-RA neurons. BiT activity inhibits sugar ingestion and promotes water ingestion. CCAP activity promotes sugar ingestion and inhibits water ingestion. CCHa2R-RA activity inhibits water ingestion.

The ISNs influence activity of several brain regions involved in feeding and nutrient homeostasis to coordinate sugar and water ingestion

Previous studies showed that the ISNs sense the hunger signal AKH and changes in hemolymph osmolality associated with thirst to correspondingly alter ISN neural activity. Increased ISN activity promotes sugar ingestion and decreases water ingestion, and decreased ISN activity decreases sugar ingestion and increases water ingestion (Jourjine, Mullaney et al., 2016). Here, we investigated how ISN activity reciprocally regulates sugar and water ingestion according to internal needs by examining the neural network modulated by the ISNs.

We found that the ISNs are predicted to synapse with 100 neurons, including projection neurons that arborize in neuroendocrine centers, SEZ interneurons, and ascending and descending neurons that likely innervate the ventral nerve cord. The majority of the ISN predicted synaptic partners are projection neurons that send arbors via the median bundle to the SMP, a neuroendocrine center (Hartenstein, 2006). This includes the cell type BiT characterized in this study that reciprocally regulates sugar and water ingestion. Local SEZ neurons downstream of the ISNs include DSOG1, which are GABAergic and inhibit consumption (Pool et al., 2014), consistent with the notion that ISN activity directly influences feeding motor programs. In addition, eight uncharacterized descending neurons are downstream of the ISNs, suggesting that they may coordinate feeding with other motor behaviors, such as locomotion or digestion. While the number of ISN postsynaptic partners precludes comprehensive functional and behavioral analysis, the restricted number of brain regions that are direct targets of the

ISNs (SMP, SEZ, and possibly ventral nerve cord) is consistent with ISN activity directly regulating neuroendocrine centers and feeding behavior.

We characterized the pathway from the second-order BiT projection neuron that oppositely regulates sugar and water consumption. We found that BiT has 93 predicted synaptic partners, including IPCs which are known to modulate food intake (Nässel & Zandawala, 2020), FLAa3/Lgr3 which have been implicated in regulating ingestion (Laturney et al., 2022, Meissner et al., 2016, Nässel et al, 2013, Yeom et al., 2021), and neurons labeled by the CCHa2R-RA-Gal4 (Deng et al., 2019) which we found regulate water ingestion. BiT downstream neurons innervate several neuropils including the SEZ, SMP, SLP, fan shaped body, and lobula. Therefore, hunger and thirst signals sensed by the ISNs fan out to modulate multiple brain regions via BiT. We speculate that the broad reach of the ISNs serves to modulate different behaviors such as sleep, reproduction, and locomotion based on the hunger or thirst state of the fly.

Communication between peptidergic neurons coordinates ingestion

Our studies demonstrate that multiple peptidergic neurons participate in regulation of sugar and water ingestion. We find that dILP3 RNAi or *amontillado* RNAi expression in the ISNs recapitulates the ISN loss-of function phenotype, arguing that the ISNs themselves are peptidergic and utilize dILP3 as the neurotransmitter that conveys hunger and thirst signals. The ISNs have increased activity upon AKH detection or low osmolality (hunger signals) (Jourjine, Mullaney et al., 2016), arguing that increased dILP3 release from the ISNs drives sucrose ingestion and limits water ingestion in hungry flies to maintain homeostasis. This conversion of an AKH signal to a

dILP3 signal resembles findings in *Drosophila* larvae, where circulating AKH binds to the AKH receptor on IPCs to release dILP3 and promote sucrose consumption (Kim & Neufeld, 2015, Palovcik et al., 1984).

The ISNs modulate activity in many neuroendocrine cells, potentially causing widespread changes in peptide release (Nässel & Zandawala, 2022, Schlegel et al., 2016). We find that ISN activation increases activity of CCAP neurons and CCHa2R-RA neurons, and BiT activation decreases the activity of IPCs. CCAP neurons are orexigenic and communicate to CCAP receptor cells, including IPCs (Zhang et al., 2022) and a subpopulation of neuropeptide F (NPF) neurons (Williams et al., 2020). While this is the first study that characterizes the CCHa2R-RA neurons, the knockin Gal4 line that labels the CCHa2R-RA neurons was generated for the RA isoform of CCHa2 receptor, suggesting that these neurons respond to CCHa2, a peptide produced in the midgut and brain that increases appetite (Deng et al., 2019, Ida et al., 2012, Reiher et al., 2011, Ren et al., 2015). Therefore, CCHa2R-RA neurons potentially integrate the hunger and thirst signals from the ISNs with CCHa2 signals from the gut. IPCs are central regulators of appetite and metabolism, receive multiple direct and indirect signals of nutrient status, and release dILP2, dILP3, and dILP5 (Nässel & Zandawala, 2020). Our finding that the ISNs communicate with multiple peptidergic systems argues that hunger and thirst signals sensed by the ISNs are integrated with other nutritive state signals sensed by ISN downstream neurons for a global assessment of the current nutritional demands of the animal.

Sugar and water ingestion remain coordinated downstream of the ISNs

Multiple neurons downstream of the ISNs bidirectionally regulate both sugar and water ingestion, arguing that they bias ingestion based on nutrient need. By studying the activation and silencing phenotypes associated with CCAP neurons, we show that acute activation promotes sugar ingestion and limits water ingestion, while silencing these neurons has the opposite effects. These findings are consistent with and expand upon previous studies showing that CCAP neurons promote feeding (Selcho et al, 2018, Williams et al., 2020). IPCs have a more complex role in regulating ingestion, with several studies showing that their acute activation limits ingestion of sucrose or food (Nässel et al., 2015, Semaniuk and Gospodaryov et al., 2018, Wang et al., 2020) and other studies suggesting the opposite (Sudhakar et al., 2020). We find that under the specific conditions of our assay, acute activation of IPCs promotes sucrose ingestion and limits water ingestion. We suspect that differing findings upon IPC manipulation may stem from differences in the deprivation state of the fly, the behavioral assay, the type and timing of neural manipulation, and the food source. As IPCs receive multiple internal state signals, it is possible that activation phenotypes depend on the current state of IPC modulation set by the internal state of the fly.

Overall, our work sheds light on neural circuit mechanisms that translate internal nutrient abundance cues into the coordinated regulation of sugar and water ingestion. We show that the hunger and thirst signals detected by the ISNs influence a network of peptidergic neurons that act in concert to prioritize ingestion of specific nutrients based on internal needs. We hypothesize that multiple internal state signals are integrated in higher brain regions such that combinations of peptides and their actions signify specific needs to drive ingestion of appropriate nutrients. As peptide signals may act at a

441 distance and may cause long-lasting neural activity state changes, studying their
442 integration over space and time is a future challenge to further illuminate homeostatic
443 feeding regulation.

444

445 ## MATERIALS AND METHODS

Key resources table		
Drosophila strains	**Source or Reference**	**Identifier**
UAS-nSynaptobrevin RNAi	Bloomington Drosophila Stock Center	BDSC 31983
UAS-dcr2	Bloomington Drosophila Stock Center	BDSC 24650
UAS-Trh RNAi	Bloomington Drosophila Stock Center	BDSC 25842
UAS-ChAT RNAi	Bloomington Drosophila Stock Center	BDSC 25856
UAS-Tbh RNAi	Bloomington Drosophila Stock Center	BDSC 27667
UAS-Hdc RNAi	Bloomington Drosophila Stock Center	BDSC 26000
UAS-VMAT RNAi	Bloomington Drosophila Stock Center	BDSC 31257
UAS-GAD1 RNAi	Bloomington Drosophila Stock Center	BDSC 28079
UAS-DDC RNAi	Bloomington Drosophila Stock Center	BDSC 27030
UAS-DVGlut RNAi	Bloomington Drosophila Stock Center	BDSC 27538
UAS-sNPF RNAi	Bloomington Drosophila Stock Center	BDSC 25867
UAS-VGAT RNAi	Bloomington Drosophila Stock Center	BDSC 41958
UAS-TDC2 RNAi	Bloomington Drosophila Stock Center	BDSC 25871
UAS-dILP1 RNAi	Bloomington Drosophila Stock Center	BDSC 32861
UAS-dILP2 RNAi	Bloomington Drosophila Stock Center	BSC 32475
UAS-dILP3 RNAi	Bloomington Drosophila Stock Center	BSC 31492
UAS-dILP4 RNAi	Bloomington Drosophila Stock Center	BDSC 33682
UAS-dILP5 RNAi	Bloomington Drosophila Stock Center	BDSC 31378
UAS-dILP6 RNAi	Bloomington Drosophila Stock Center	BDSC 33684
UAS-dILP7 RNAi	Bloomington Drosophila Stock Center	BDSC 32862
UAS-amon RNAi	Bloomington Drosophila Stock Center	BDSC 29009
ISN-Gal4 (VT011155-Gal4)	FlyLight, Janelia Research Campus	Fly Light ID 54404

ISN-LexA (GMR34G02-LexA)	Bloomington Drosophila Stock Center	BDSC 54138
UAS-myrGFP.QUAS-mtdTomato-3xHA; trans-Tango	Bloomington Drosophila Stock Center	BDSC 77124
VT002073-Gal4.AD	Bloomington Drosophila Stock Center	BDSC 71871
VT040568-Gal4.DBD	Bloomington Drosophila Stock Center	BDSC 72902
UAS-csChrimson.mVenus	Bloomington Drosophila Stock Center	BDSC 55134
LexAop-ChrimsonR.mCherry	Gift from Jayaraman Lab	
UAS-ArcLight	Bloomington Drosophila Stock Center	BDSC 51056
Empty split	Bloomington Drosophila Stock Center	BDSC 79603
ppk28-Gal4	Cameron et al 2010.	BDSC 93020
Gr5a-Gal4	Chyb et al 2003.	BDSC 57592, 57591
CCha2R-RA-Gal4	Bloomington Drosophila Stock Center	BDSC 84603
LexAop-CsChrimson.tdTomato (III)	Bloomington Drosophila Stock Center	BDSC 82183
UAS-GCaMP6s (III)	Bloomington Drosophila Stock Center	BDSC 42749
20XUAS-GCaMP7b	Bloomington Drosophila Stock Center	BDSC 79029
CCAP-Gal4 (II)	Bloomington Drosophila Stock Center	BDSC 25685
CCAP-Gal4 (III)	Bloomington Drosophila Stock Center	BDSC 25686
CCHa2R-RA-LexA	Bloomington Drosophila Stock Center	BDSC 84363
dILP2-LexA	Li and Gong 2015.	

Fly husbandry

All experiments and screening were carried out with adult *D. melanogaster* females reared on standard cornmeal-agar-molasses medium, at 25°C, 65-70% humidity, on a 12 hr light: 12 hr dark cycle. Flies used in optogenetic assays were reared on food containing 0.25mM all-trans-retinal (Sigma-AldrichSigna-Aldrich) in darkness, before and after eclosion.

Temporal consumption assay (TCA)

Flies were anesthetized using CO_2 and then fixed to a glass slide with nail polish. Flies recovered for 2 hours in a humidified box if testing for sucrose ingestion, or in a desiccated box with Drierite if testing for water ingestion. Immediately before testing for sucrose ingestion, flies were given water until they no longer responded to 3 consecutive water presentations. In testing, flies were presented with the tastant (water or 1M sucrose) 10 times and consumption time was manually recorded. All experiments were done in a dark, temperature- and humidity-controlled room. IR lights and IR cameras were used to conduct experiments in the dark. All water tests were done in the morning and all sugar tests were done in the afternoon. For optogenetic activation experiments, we expressed the light activated ion channel Chrimson in the neurons of interest and activated these neurons using a 635nm laser (Laserglow). For silencing experiments, we expressed RNAi against nSynaptobrevin in neurons of interest.

In vivo calcium imaging

Calcium imaging studies were carried out as described in Shiu, Sterne et al. (2022). Mated female flies were dissected for calcium imaging studies 5-14 days post-eclosion. Flies were briefly anesthetized with ice and placed in a custom plastic holder at the neck to isolate the head from the rest of the body. The head was then immobilized using UV glue, the proboscis was immobilized using wax, and the esophagus was cut to provide unobstructed imaging access to the SEZ. All flies imaged were sated. *In vivo* calcium imaging with optogenetic activation was performed in a 2-photon microscope using a Scientifica Hyperscope with resonant scanning, a piezo drive, and a 20x water immersion objective (NA = 1.0) with 1.8-3x digital zoom, depending on the cell type

imaged. Calcium responses were recorded with a 920 nm laser and optogenetic stimulation was achieved with a 660 nm LED. 2s LED stimulation paradigm: 20s off, 2s on, 30s off, 2s on, 30s off. 30s LED stimulation paradigm: 20s off, (1s on, 1s off) x 15, 60s off. For the 2s LED stimulation, 80 stacks of 20 z slices of 4-5 µm were acquired at 0.667 Hz. For the 30s stimulation, 125 stacks of 20 z slices of 4-5 µm were acquired at 0.667 Hz. Analysis was done on max-z projections of the 20 z slices. %ΔF/F = 100*((Ft-F0)/F0), where Ft is the fluorescence of the Neuron ROI - the Background ROI at each timepoint and F0 is the mean Ft for the 23 time points prior to stimulus onset. Quantification was carried out in GraphPad Prism. A mean fluorescence intensity for LED off and LED on was calculated for each fly. For the 2s LED stimulation, mean intensity for LED off was calculated for 5 timepoints immediately before LED exposure and mean intensity for LED on was calculated for 5 timepoints during LED exposure. For the 30s stimulation, mean intensity for LED off was calculated for 28 timepoints immediately before LED exposure and mean intensity for LED on was calculated for 28 timepoints during LED exposure. Paired t-test or paired Wilcoxon test was performed. ROI for CCHa2R-RA imaging was CCHa2R-RA neurites in SEZ. ROI for CCAP imaging was CCAP neurites. ROI for IPC imaging was all IPC somas.

***In vivo* voltage imaging**

Voltage imaging studies were carried out exactly as calcium imaging studies described above. ROI for BiT imaging was BiT soma.

Immunohistochemistry

All brain and CNS dissections and immunostaining (unless directly addressed) were carried out as described (https://www.janelia.org/project-team/flylight/protocols, 'IHC-Anti-GFP') substituting the below antibodies and eschewing the pre-embedding fixation steps. Ethanol dehydration and DPX mounting was carried out as described (https://www.janelia.org/project-team/flylight/protocols, 'DPX Mounting').

Primary antibodies:

- mouse α-Brp (nc82, DSHB, University of Iowa, USA) at 1:40
- chicken α-GFP (Invitrogen, A10262) at 1:1000
- rabbit α-dsRed (Takara, Living Colors 632496) at 1:1000

Secondary antibodies:

- goat α-mouse AF647 (Invitrogen, A21236) at 1:500
- goat α-chicken AF488 (Life Technologies, A11039) at 1:1000
- goat α-rabbit AF568 (Invitrogen, A21236) at 1:1000

Images were acquired with a Zeiss LSM 880 NLO AxioExaminer with Airyscan and Coherent Chameleon Vision or Zeiss LSM 780 Laser Scanning Confocal Microscope at the Berkeley Molecular Imaging Center with a Plan-Apochromat 20x/1.0 W, 40x W, 40x/1.4 oil, or 63x/1.4 oil objective. Images were prepared in Fiji.

Electron microscopy neural reconstructions and connectivity

Neurons were reconstructed in a serial section transmission electron volume (Full Adult Female Brain, Zheng and Lauritzen et al., 2018) using the CATMAID software (Saalfeld et al., 2009). Fully manual reconstructions were generated by following the branches of

the neuron and marking the center of each branch, thereby creating a 'skeleton' of each neuron. In addition to fully manual reconstructions, segments of an automated segmentation (Li et al., 2019) were proofread and expanded to generate complete reconstructions. In addition to the skeleton tracing, new chemical synapses were also annotated as previously described (Zheng and Lauritzen et al. 2018). Downstream synaptic targets of the ISNs and BiT were then traced out from these additional locations using both manual and assisted tracing techniques as described above. Neurons traced in CATMAID, including ISNs and BiT, were all located in Flywire (flywire.ai), which uses the same EM electron microscopy dataset (Zheng and Lauritzen et al. 2018). To identify synaptic partners, we used connectome annotation versioning engine (CAVE, Buhmann et al. 2021, Heinrich et al. 2018) using a cleft score cutoff of 50 to generate synapses of relatively high confidence (Heinrich et al. 2018; Baker et al., 2022). FAFB neural reconstructions were visualized using NAVis (Copyright 2018, Philipp Schlegel), which is based on natverse (Bates et al., 2020).

BiT split-Gal4 generation

We created a color depth max intensity projection (CDM) mask of BiT reconstructed EM skeleton and used CDM mask searching (Otsuna et al., 2018) to find enhancers whose expression patterns seemed to include the desired cell type using MCFO (Nern et al., 2015) screening of subsets of the Janelia Research Campus and Vienna Tile Gal4 collections. Construction of stable split-Gal4 lines was performed as previously described (Dionne et al., 2018, Sterne et al., 2020). Immunohistochemistry and confocal imaging was used to determine successful split-Gal4 combinations.

Identification of GAL4 lines from EM reconstructions

Visual inspection of Gal4 collections was used to determine cell type. Images of potential Gal4 lines were skeletonized in FIJI, converted into .swc format using natverse (Bates et al., 2021), and uploaded to Flywire using the Flywire Gateway. This generated pointclouds that were used to identify the neurons of interest. As Flywire permits exhaustive searching of neurons in an area, we examined all neurons in the region of interest to conclusively identify our neuron of interest.

Statistical analysis

Statistical tests were performed in GraphPad Prism. For all group comparisons, data was first tested for normality with the KS normality test (alpha = 0.05). If all groups passed then groups were compared with a parametric test, but if at least one group did not pass, groups were compared with a non-parametric version. All statistical tests, significance levels, and number of data points (N) are specified in the figure legend. All datasets from optogenetic behavior assays were normalized within each genotype. To generate this normalized dataset, data from females within the no light condition was averaged, creating a “no-light mean” for each genotype. This value was subtracted from each individual female within the light condition of the corresponding genotype. This dataset was then graphed, and statistical analyses were performed as outlined above.

ACKNOWLEDGEMENTS

569 Members of the Scott lab provided contributions to experimental design, data analysis,
570 and manuscript preparation. This work was supported by NIH R01GM128209 (K.S.),
571 R01GM128209 Diversity Supplement (A.G.S.), UC LEADs fellowship (A.D.T.) and
572 International Fellowship for CONICET Researchers (G.P.). Neuronal reconstruction for
573 this project took place in a collaborative CATMAID environment in which 27 labs are
574 participating to build connectomes for specific circuits. Development and administration
575 of the FAFB tracing environment and analysis tools were funded in part by National
576 Institutes of Health BRAIN Initiative grant 1RF1MH120679-01 to Davi Bock and Greg
577 Jefferis, with software development effort and administrative support provided by Tom
578 Kazimiers (Kazmos GmbH) and Eric Perlman (Yikes LLC). We thank Peter Li, Viren
579 Jain and colleagues at Google Research for sharing the automatic segmentation (Li et
580 al., 2019). Tracing in Cambridge was supported by Wellcome Trust (203261/Z/16/Z)
581 and ERC (649111) awards to G. Jefferis. Neurons were also reconstructed and
582 proofread in FlyWire, where we also identified pre- and postsynaptic partners. We
583 acknowledge the Princeton FlyWire team and members of the Murthy and Seung labs
584 for development and maintenance of FlyWire (supported by BRAIN initiative grant
585 MH117815 to Murthy and Seung). In addition to our tracing efforts in CATMAID and
586 proofreading in FlyWire, the following labs greatly contributed to the proofreading in
587 FlyWire of the neurons characterized in this study: Murthy and Seung Labs (76.06%),
588 Jefferis Lab (13.57%) and Jinseop Kim Lab (7.21%). We are appreciative of the
589 proofreading contributed by other labs including the Anderson, Bock, Dacks, Dickson,
590 Huetteroth, Pankratz, Seeds/Hampel, Selcho, Simpson, Waddell, Wilson and Wolf
591 Labs, and Janelia tracers (Supplementary Table 1, Supplementary Table 2,

Supplementary Table 3). Vivek Jayaraman provided unpublished fly lines used in this study. We thank Stefanie Engert for tracing two ISNs in CATMAID, Zepeng Yao for identifying CCHa2R-RA neurons, Phil Shiu for identifying DSOG1 neurons, and Amanda Abusaif for her tracing and proofreading efforts. Confocal imaging experiments were conducted at the CRL Molecular Imaging Center, RRID:SCR_017852, supported by NSF DBI-1041078 and the Helen Wills Neuroscience Institute. We thank Holly Aaron and Feather Ives for microscopy training and support.

AUTHOR CONTRIBUTIONS

A.G.S. and K.S. conceived and designed the study and wrote the manuscript. A.G.S performed the FAFB circuit building and cell identification, BiT split-Gal4 creation, functional imaging experiments, immunohistochemistry, and data analysis. G.P. performed behavior experiments and BiT split-Gal4 creation. N.J performed the ISN neurotransmitter RNAi screen. A.D.T. traced ISNs and BiT in CATMAID.

COMPETING INTERESTS

The authors declare no competing interests.

REFERENCES

Aponte, Y., Atasoy, D., & Sternson, S. M. (2011). AGRP neurons are sufficient to orchestrate feeding behavior rapidly and without training. *Nat Neurosci*, *14*(3), 351-355. https://doi.org/10.1038/nn.2739

Badisco, L., Van Wielendaele, P., & Vanden Broeck, J. (2013). Eat to reproduce: a key role for the insulin signaling pathway in adult insects. *Front Physiol*, *4*, 202. https://doi.org/10.3389/fphys.2013.00202

618 Baker, C. A., McKellar, C., Pang, R., Nern, A., Dorkenwald, S., Pacheco, D. A.,
619 Eckstein, N., Funke, J., Dickson, B. J., & Murthy, M. (2022). Neural network
620 organization for courtship-song feature detection in Drosophila. *Curr Biol*, *32*(15),
621 3317-3333 e3317. https://doi.org/10.1016/j.cub.2022.06.019
622 Bates, A. S., Manton, J. D., Jagannathan, S. R., Costa, M., Schlegel, P., Rohlfing, T., &
623 Jefferis, G. S. (2020). The natverse, a versatile toolbox for combining and
624 analysing neuroanatomical data. *Elife*, *9*. https://doi.org/10.7554/eLife.53350
625 Biglou, S. G., Bendena, W. G., & Chin-Sang, I. (2021). An overview of the insulin
626 signaling pathway in model organisms Drosophila melanogaster and
627 Caenorhabditis elegans. *Peptides*, *145*, 170640.
628 https://doi.org/10.1016/j.peptides.2021.170640
629 Brogiolo, W., Stocker, H., Ikeya, T., Rintelen, F., Fernandez, R., & Hafen, E. (2001). An
630 evolutionarily conserved function of the Drosophila insulin receptor and insulin-
631 like peptides in growth control. *Current biology*, *11*(4), 213-221.
632 Buhmann, J., Sheridan, A., Malin-Mayor, C., Schlegel, P., Gerhard, S., Kazimiers, T.,
633 Krause, R., Nguyen, T. M., Heinrich, L., Lee, W. A., Wilson, R., Saalfeld, S.,
634 Jefferis, G., Bock, D. D., Turaga, S. C., Cook, M., & Funke, J. (2021). Automatic
635 detection of synaptic partners in a whole-brain Drosophila electron microscopy
636 data set. *Nat Methods*, *18*(7), 771-774. https://doi.org/10.1038/s41592-021-
637 01183-7
638 Burnett, C. J., Li, C., Webber, E., Tsaousidou, E., Xue, S. Y., Bruning, J. C., & Krashes,
639 M. J. (2016). Hunger-Driven Motivational State Competition. *Neuron*, *92*(1), 187-
640 201. https://doi.org/10.1016/j.neuron.2016.08.032
641 Cannell, E., Dornan, A. J., Halberg, K. A., Terhzaz, S., Dow, J. A. T., & Davies, S. A.
642 (2016). The corticotropin-releasing factor-like diuretic hormone 44 (DH44) and
643 kinin neuropeptides modulate desiccation and starvation tolerance in Drosophila
644 melanogaster. *Peptides*, *80*, 96-107.
645 https://doi.org/10.1016/j.peptides.2016.02.004
646 Chen, C., Jack, J., & Garofalo, R. S. (1996). The Drosophila insulin receptor is required
647 for normal growth. *Endocrinology*, *137*(3), 846-856.
648 Chen, T. W., Wardill, T. J., Sun, Y., Pulver, S. R., Renninger, S. L., Baohan, A.,
649 Schreiter, E. R., Kerr, R. A., Orger, M. B., Jayaraman, V., Looger, L. L., Svoboda,
650 K., & Kim, D. S. (2013). Ultrasensitive fluorescent proteins for imaging neuronal
651 activity. *Nature*, *499*(7458), 295-300. https://doi.org/10.1038/nature12354
652 Claeys, I., Simonet, G., Poels, J., Van Loy, T., Vercammen, L., De Loof, A., & Broeck, J.
653 V. (2002). Insulin-related peptides and their conserved signal transduction
654 pathway. *Peptides*, *23*(4), 807-816.
655 Clancy, D. J., Gems, D., Harshman, L. G., Oldham, S., Stocker, H., Hafen, E., Leevers,
656 S. J., & Partridge., L. (2001). Extension of Life-Span by Loss of CHICO, a
657 Drosophila Insulin Receptor Substrate Protein. *Science*, *292*(5514), 104-106.
658 Deng, B., Li, Q., Liu, X., Cao, Y., Li, B., Qian, Y., Xu, R., Mao, R., Zhou, E., Zhang, W.,
659 Huang, J., & Rao, Y. (2019). Chemoconnectomics: Mapping Chemical
660 Transmission in Drosophila. *Neuron*, *101*(5), 876-893 e874.
661 https://doi.org/10.1016/j.neuron.2019.01.045
662 Dethier, V. G. (1976). The hungry fly: A physiological study of the behavior associated
663 with feeding.

664 Dionne, H., Hibbard, K. L., Cavallaro, A., Kao, J. C., & Rubin, G. M. (2018). Genetic
665 Reagents for Making Split-GAL4 Lines in Drosophila. *Genetics*, *209*(1), 31-35.
666 https://doi.org/10.1534/genetics.118.300682
667 Dorkenwald, S., McKellar, C. E., Macrina, T., Kemnitz, N., Lee, K., Lu, R., Wu, J.,
668 Popovych, S., Mitchell, E., & Nehoran, B. (2022). FlyWire: online community for
669 whole-brain connectomics. *Nature methods*, *19*(1), 119-128.
670 Eckstein, N., Bates, A. S., Du, M., Hartenstein, V., Jefferis, G. S. X. E., & Funke, J.
671 (2020). Neurotransmitter Classification from Electron
672 Microscopy Images at Synaptic Sites in Drosophila. *bioRxiv*.
673 https://doi.org/10.1101/2020.06.12.148775
674 Eiselt, A. K., Chen, S., Chen, J., Arnold, J., Kim, T., Pachitariu, M., & Sternson, S. M.
675 (2021). Hunger or thirst state uncertainty is resolved by outcome evaluation in
676 medial prefrontal cortex to guide decision-making. *Nat Neurosci*, *24*(7), 907-912.
677 https://doi.org/10.1038/s41593-021-00850-4
678 Fernandez, R., Tabarini, D., Azpiazu, N., Frasch, M., & Schlessinger, J. (1995). The
679 Drosophila insulin receptor homolog: a gene essential for embryonic
680 development encodes two receptor isoforms with different signaling potential.
681 *EMBO J*, *14*(14), 3373-3384. https://doi.org/10.1002/j.1460-2075.1995.tb07343.x
682 Gáliková, M., Diesner, M., Klepsatel, P., Hehlert, P., Xu, Y., Bickmeyer, I., Predel, R., &
683 Kuhnlein, R. P. (2015). Energy Homeostasis Control in Drosophila Adipokinetic
684 Hormone Mutants. *Genetics*, *201*(2), 665-683.
685 https://doi.org/10.1534/genetics.115.178897
686 Gáliková, M., Dircksen, H., & Nässel, D. R. (2018). The thirsty fly: Ion transport peptide
687 (ITP) is a novel endocrine regulator of water homeostasis in Drosophila. *PLoS*
688 *Genet*, *14*(8), e1007618. https://doi.org/10.1371/journal.pgen.1007618
689 Garofalo, R. S. (2002). Genetic analysis of insulin signaling in Drosophila. *Trends in*
690 *Endocrinology & Metabolism*, *13*(4), 156-162.
691 Gizowski, C., & Bourque, C. W. (2018). The neural basis of homeostatic and
692 anticipatory thirst. *Nat Rev Nephrol*, *14*(1), 11-25.
693 https://doi.org/10.1038/nrneph.2017.149
694 Gordon, M. D., & Scott, K. (2009). Motor control in a Drosophila taste circuit. *Neuron*,
695 *61*(3), 373-384. https://doi.org/10.1016/j.neuron.2008.12.033
696 Graham, M., Shutter, J. R., Sarmiento, U., Sarosi, I., & Stark, K. L. (1997).
697 Overexpression of Agrt leads to obesity in transgenic mice. *Nature genetics*,
698 *17*(3), 273-274.
699 Grönke, S., Clarke, D. F., Broughton, S., Andrews, T. D., & Partridge, L. (2010).
700 Molecular evolution and functional characterization of Drosophila insulin-like
701 peptides. *PLoS Genet*, *6*(2), e1000857.
702 https://doi.org/10.1371/journal.pgen.1000857
703 Hartenstein, V. (2006). The neuroendocrine system of invertebrates: a developmental
704 and evolutionary perspective. *J Endocrinol*, *190*(3), 555-570.
705 https://doi.org/10.1677/joe.1.06964
706 Heinrich, L., Funke, J., Pape, C., Nunez-Iglesias, J., & Saalfeld, S. (2018). Synaptic cleft
707 segmentation in non-isotropic volume electron microscopy of the complete
708 drosophila brain. Medical Image Computing and Computer Assisted

Intervention–MICCAI 2018: 21st International Conference, Granada, Spain, September 16-20, 2018, Proceedings, Part II 11,

Ida, T., Takahashi, T., Tominaga, H., Sato, T., Sano, H., Kume, K., Ozaki, M., Hiraguchi, T., Shiotani, H., Terajima, S., Nakamura, Y., Mori, K., Yoshida, M., Kato, J., Murakami, N., Miyazato, M., Kangawa, K., & Kojima, M. (2012). Isolation of the bioactive peptides CCHamide-1 and CCHamide-2 from Drosophila and their putative role in appetite regulation as ligands for G protein-coupled receptors. *Front Endocrinol (Lausanne)*, *3*, 177. https://doi.org/10.3389/fendo.2012.00177

Jin, L., Han, Z., Platisa, J., Wooltorton, J. R., Cohen, L. B., & Pieribone, V. A. (2012). Single action potentials and subthreshold electrical events imaged in neurons with a fluorescent protein voltage probe. *Neuron*, *75*(5), 779-785. https://doi.org/10.1016/j.neuron.2012.06.040

Jourjine, N. (2017). Hunger and thirst interact to regulate ingestive behavior in flies and mammals. *BioEssays*, *39*(5). https://doi.org/10.1002/bies.201600261

Jourjine, N., Mullaney, B. C., Mann, K., & Scott, K. (2016). Coupled Sensing of Hunger and Thirst Signals Balances Sugar and Water Consumption. *Cell*, *166*(4), 855-866. https://doi.org/10.1016/j.cell.2016.06.046

Kim, J., & Neufeld, T. P. (2015). Dietary sugar promotes systemic TOR activation in Drosophila through AKH-dependent selective secretion of Dilp3. *Nat Commun*, *6*, 6846. https://doi.org/10.1038/ncomms7846

Klapoetke, N. C., Murata, Y., Kim, S. S., Pulver, S. R., Birdsey-Benson, A., Cho, Y. K., Morimoto, T. K., Chuong, A. S., Carpenter, E. J., Tian, Z., Wang, J., Xie, Y., Yan, Z., Zhang, Y., Chow, B. Y., Surek, B., Melkonian, M., Jayaraman, V., Constantine-Paton, M., . . . Boyden, E. S. (2014). Independent optical excitation of distinct neural populations. *Nat Methods*, *11*(3), 338-346. https://doi.org/10.1038/nmeth.2836

Landayan, D., Wang, B. P., Zhou, J., & Wolf, F. W. (2021). Thirst interneurons that promote water seeking and limit feeding behavior in Drosophila. *Elife*, *10*. https://doi.org/10.7554/eLife.66286

Laturney, M., Sterne, G. R., & Scott, K. (2022). Mating activates neuroendocrine pathways signaling hunger in Drosophila females. *bioRxiv*. https://doi.org/10.1101/2022.10.19.512959

Lee, Y. J., Yang, C. P., Miyares, R. L., Huang, Y. F., He, Y., Ren, Q., Chen, H. M., Kawase, T., Ito, M., Otsuna, H., Sugino, K., Aso, Y., Ito, K., & Lee, T. (2020). Conservation and divergence of related neuronal lineages in the Drosophila central brain. *Elife*, *9*. https://doi.org/10.7554/eLife.53518

Li, P. H., Lindsey, L. F., Januszewski, M., Tyka, M., Maitin-Shepard, J., Blakely, T., & Jain, V. (2019). Automated Reconstruction of a Serial-Section EM Drosophila Brain with Flood-Filling Networks and Local Realignment. *Microscopy and Microanalysis*, *25*(S2), 1364-1365. https://doi.org/10.1017/s1431927619007554

Lin, S., Owald, D., Chandra, V., Talbot, C., Huetteroth, W., & Waddell, S. (2014). Neural correlates of water reward in thirsty Drosophila. *Nat Neurosci*, *17*(11), 1536-1542. https://doi.org/10.1038/nn.3827

753 Liu, W. W., & Wilson, R. I. (2013). Glutamate is an inhibitory neurotransmitter in the
754 Drosophila olfactory system. *Proc Natl Acad Sci U S A*, *110*(25), 10294-10299.
755 https://doi.org/10.1073/pnas.1220560110
756 Meissner, G. W., Luo, S. D., Dias, B. G., Texada, M. J., & Baker, B. S. (2016). Sex-
757 specific regulation of Lgr3 in Drosophila neurons. *Proc Natl Acad Sci U S A*,
758 *113*(9), E1256-1265. https://doi.org/10.1073/pnas.1600241113
759 Min, S., Chae, H. S., Jang, Y. H., Choi, S., Lee, S., Jeong, Y. T., Jones, W. D., Moon, S.
760 J., Kim, Y. J., & Chung, J. (2016). Identification of a Peptidergic Pathway Critical
761 to Satiety Responses in Drosophila. *Curr Biol*, *26*(6), 814-820.
762 https://doi.org/10.1016/j.cub.2016.01.029
763 Nässel, D. R., Kubrak, O. I., Liu, Y., Luo, J., & Lushchak, O. V. (2013). Factors that
764 regulate insulin producing cells and their output in Drosophila. *Front Physiol*, *4*,
765 252. https://doi.org/10.3389/fphys.2013.00252
766 Nässel, D. R., Liu, Y., & Luo, J. (2015). Insulin/IGF signaling and its regulation in
767 Drosophila. *Gen Comp Endocrinol*, *221*, 255-266.
768 https://doi.org/10.1016/j.ygcen.2014.11.021
769 Nässel, D. R., & Vanden Broeck, J. (2016). Insulin/IGF signaling in Drosophila and other
770 insects: factors that regulate production, release and post-release action of the
771 insulin-like peptides. *Cell Mol Life Sci*, *73*(2), 271-290.
772 https://doi.org/10.1007/s00018-015-2063-3
773 Nässel, D. R., & Zandawala, M. (2020). Hormonal axes in Drosophila: regulation of
774 hormone release and multiplicity of actions. *Cell Tissue Res*, *382*(2), 233-266.
775 https://doi.org/10.1007/s00441-020-03264-z
776 Nässel, D. R., & Zandawala, M. (2022). Endocrine cybernetics: neuropeptides as
777 molecular switches in behavioural decisions. *Open Biol*, *12*(7), 220174.
778 https://doi.org/10.1098/rsob.220174
779 Nern, A., Pfeiffer, B. D., & Rubin, G. M. (2015). Optimized tools for multicolor stochastic
780 labeling reveal diverse stereotyped cell arrangements in the fly visual system.
781 *Proc Natl Acad Sci U S A*, *112*(22), E2967-2976.
782 https://doi.org/10.1073/pnas.1506763112
783 Ohhara, Y., Kobayashi, S., Yamakawa-Kobayashi, K., & Yamanaka, N. (2018). Adult-
784 specific insulin-producing neurons in Drosophila melanogaster. *J Comp Neurol*,
785 *526*(8), 1351-1367. https://doi.org/10.1002/cne.24410
786 Orchard, I. (1987). Adipokinetic hormones—an update. *Journal of insect physiology*,
787 *33*(7), 451-463.
788 Otsuna, H., Ito, M., & Kawase, T. (2018). Color depth MIP mask search: a new tool to
789 expedite SplitGAL4 creation. *bioRxiv*. https://doi.org/10.1101/318006
790 Palovcik, R. A., Phillips, M. I., Kappy, M. S., & Raizada, M. K. (1984). Insulin inhibits
791 pyramidal neurons in hippocampal slices. *Brain research*, *309*(1), 187-191.
792 Pfeiffer, B. D., Jenett, A., Hammonds, A. S., Ngo, T.-T. B., Misra, S., Murphy, C., Scully,
793 A., Carlson, J. W., Wan, K. H., & Laverty, T. R. (2008). Tools for neuroanatomy
794 and neurogenetics in Drosophila. *Proceedings of the National Academy of*
795 *Sciences*, *105*(28), 9715-9720.
796 Pool, A. H., Kvello, P., Mann, K., Cheung, S. K., Gordon, M. D., Wang, L., & Scott, K.
797 (2014). Four GABAergic interneurons impose feeding restraint in Drosophila.
798 *Neuron*, *83*(1), 164-177. https://doi.org/10.1016/j.neuron.2014.05.006

Qi, W., Wang, G., & Wang, L. (2021). A novel satiety sensor detects circulating glucose and suppresses food consumption via insulin-producing cells in Drosophila. *Cell Res*, *31*(5), 580-588. https://doi.org/10.1038/s41422-020-00449-7

Reiher, W., Shirras, C., Kahnt, J., Baumeister, S., Isaac, R. E., & Wegener, C. (2011). Peptidomics and peptide hormone processing in the Drosophila midgut. *J Proteome Res*, *10*(4), 1881-1892. https://doi.org/10.1021/pr101116g

Ren, G. R., Hauser, F., Rewitz, K. F., Kondo, S., Engelbrecht, A. F., Didriksen, A. K., Schjott, S. R., Sembach, F. E., Li, S., Sogaard, K. C., Sondergaard, L., & Grimmelikhuijzen, C. J. (2015). CCHamide-2 Is an Orexigenic Brain-Gut Peptide in Drosophila. *PLoS One*, *10*(7), e0133017. https://doi.org/10.1371/journal.pone.0133017

Saalfeld, S., Cardona, A., Hartenstein, V., & Tomancak, P. (2009). CATMAID: collaborative annotation toolkit for massive amounts of image data. *Bioinformatics*, *25*(15), 1984-1986. https://doi.org/10.1093/bioinformatics/btp266

Sano, H., Nakamura, A., Texada, M. J., Truman, J. W., Ishimoto, H., Kamikouchi, A., Nibu, Y., Kume, K., Ida, T., & Kojima, M. (2015). The Nutrient-Responsive Hormone CCHamide-2 Controls Growth by Regulating Insulin-like Peptides in the Brain of Drosophila melanogaster. *PLoS Genet*, *11*(5), e1005209. https://doi.org/10.1371/journal.pgen.1005209

Schlegel, P., Texada, M. J., Miroschnikow, A., Schoofs, A., Huckesfeld, S., Peters, M., Schneider-Mizell, C. M., Lacin, H., Li, F., Fetter, R. D., Truman, J. W., Cardona, A., & Pankratz, M. J. (2016). Synaptic transmission parallels neuromodulation in a central food-intake circuit. *Elife*, *5*. https://doi.org/10.7554/eLife.16799

Scott, K., Brady Jr, R., Cravchik, A., Morozov, P., Rzhetsky, A., Zuker, C., & Axel, R. (2001). A chemosensory gene family encoding candidate gustatory and olfactory receptors in Drosophila. *Cell*, *104*(5), 661-673.

Selcho, M., Muhlbauer, B., Hensgen, R., Shiga, S., Wegener, C., & Yasuyama, K. (2018). Anatomical characterization of PDF-tri neurons and peptidergic neurons associated with eclosion behavior in Drosophila. *J Comp Neurol*, *526*(8), 1307-1328. https://doi.org/10.1002/cne.24408

Semaniuk, U. V., Gospodaryov, D. V., Feden'ko, K. M., Yurkevych, I. S., Vaiserman, A. M., Storey, K. B., Simpson, S. J., & Lushchak, O. (2018). Insulin-Like Peptides Regulate Feeding Preference and Metabolism in Drosophila. *Front Physiol*, *9*, 1083. https://doi.org/10.3389/fphys.2018.01083

Shahid, S., Shi, Y., Yang, C., Li, J., Ali, M. Y., Smagghe, G., & Liu, T. X. (2021). CCHamide2-receptor regulates feeding behavior in the pea aphid, Acyrthosiphon pisum. *Peptides*, *143*, 170596. https://doi.org/10.1016/j.peptides.2021.170596

Shiu, P. K., Sterne, G. R., Engert, S., Dickson, B. J., & Scott, K. (2022). Taste quality and hunger interactions in a feeding sensorimotor circuit. *Elife*, *11*. https://doi.org/10.7554/eLife.79887

Siekhaus, D. E., & Fuller, R. S. (1999). A role for amontillado, the Drosophilahomolog of the neuropeptide precursor processing protease PC2, in triggering hatching behavior. *Journal of Neuroscience*, *19*(16), 6942-6954.

Söderberg, J. A., Carlsson, M. A., & Nässel, D. R. (2012). Insulin-Producing Cells in the Drosophila Brain also Express Satiety-Inducing Cholecystokinin-Like Peptide,

Drosulfakinin. *Front Endocrinol (Lausanne)*, *3*, 109. https://doi.org/10.3389/fendo.2012.00109

Sterne, G. R., Otsuna, H., Dickson, B. J., & Scott, K. (2021). Classification and genetic targeting of cell types in the primary taste and premotor center of the adult Drosophila brain. *Elife*, *10*. https://doi.org/10.7554/eLife.71679

Sternson, S. M., Nicholas Betley, J., & Cao, Z. F. (2013). Neural circuits and motivational processes for hunger. *Curr Opin Neurobiol*, *23*(3), 353-360. https://doi.org/10.1016/j.conb.2013.04.006

Sudhakar, S. R., Pathak, H., Rehman, N., Fernandes, J., Vishnu, S., & Varghese, J. (2020). Insulin signalling elicits hunger-induced feeding in Drosophila. *Dev Biol*, *459*(2), 87-99. https://doi.org/10.1016/j.ydbio.2019.11.013

Talay, M., Richman, E. B., Snell, N. J., Hartmann, G. G., Fisher, J. D., Sorkac, A., Santoyo, J. F., Chou-Freed, C., Nair, N., Johnson, M., Szymanski, J. R., & Barnea, G. (2017). Transsynaptic Mapping of Second-Order Taste Neurons in Flies by trans-Tango. *Neuron*, *96*(4), 783-795 e784. https://doi.org/10.1016/j.neuron.2017.10.011

Tatar, M., Kopelman, A., Epstein, D., Tu, M.-P., Yin, C.-M., & Garofalo, R. (2001). A mutant Drosophila insulin receptor homolog that extends life-span and impairs neuroendocrine function. *Science*, *292*(5514), 107-110.

van den Pol, A. N. (2012). Neuropeptide transmission in brain circuits. *Neuron*, *76*(1), 98-115. https://doi.org/10.1016/j.neuron.2012.09.014

Veenstra, J. A., Agricola, H. J., & Sellami, A. (2008). Regulatory peptides in fruit fly midgut. *Cell Tissue Res*, *334*(3), 499-516. https://doi.org/10.1007/s00441-008-0708-3

Wang, P., Jia, Y., Liu, T., Jan, Y. N., & Zhang, W. (2020). Visceral Mechano-sensing Neurons Control Drosophila Feeding by Using Piezo as a Sensor. *Neuron*, *108*(4), 640-650 e644. https://doi.org/10.1016/j.neuron.2020.08.017

Wang, Z., Singhvi, A., Kong, P., & Scott, K. (2004). Taste representations in the Drosophila brain. *Cell*, *117*(7), 981-991. https://doi.org/10.1016/j.cell.2004.06.011

Watts, A. G., & Boyle, C. N. (2010). The functional architecture of dehydration-anorexia. *Physiol Behav*, *100*(5), 472-477. https://doi.org/10.1016/j.physbeh.2010.04.010

Williams, M. J., Akram, M., Barkauskaite, D., Patil, S., Kotsidou, E., Kheder, S., Vitale, G., Filaferro, M., Blemings, S. W., Maestri, G., Hazim, N., Vergoni, A. V., & Schioth, H. B. (2020). CCAP regulates feeding behavior via the NPF pathway in Drosophila adults. *Proc Natl Acad Sci U S A*, *117*(13), 7401-7408. https://doi.org/10.1073/pnas.1914037117

Wu, M., Nern, A., Williamson, W. R., Morimoto, M. M., Reiser, M. B., Card, G. M., & Rubin, G. M. (2016). Visual projection neurons in the Drosophila lobula link feature detection to distinct behavioral programs. *Elife*, *5*. https://doi.org/10.7554/eLife.21022

Yapici, N., Cohn, R., Schusterreiter, C., Ruta, V., & Vosshall, L. B. (2016). A Taste Circuit that Regulates Ingestion by Integrating Food and Hunger Signals. *Cell*, *165*(3), 715-729. https://doi.org/10.1016/j.cell.2016.02.061

Yeom, E., Shin, H., Yoo, W., Jun, E., Kim, S., Hong, S. H., Kwon, D. W., Ryu, T. H., Suh, J. M., Kim, S. C., Lee, K. S., & Yu, K. (2021). Tumour-derived Dilp8/INSL3

induces cancer anorexia by regulating feeding neuropeptides via Lgr3/8 in the brain. *Nat Cell Biol*, *23*(2), 172-183. https://doi.org/10.1038/s41556-020-00628-z

Yoshinari, Y., Kosakamoto, H., Kamiyama, T., Hoshino, R., Matsuoka, R., Kondo, S., Tanimoto, H., Nakamura, A., Obata, F., & Niwa, R. (2021). The sugar-responsive enteroendocrine neuropeptide F regulates lipid metabolism through glucagon-like and insulin-like hormones in Drosophila melanogaster. *Nat Commun*, *12*(1), 4818. https://doi.org/10.1038/s41467-021-25146-w

Yu, H. H., Awasaki, T., Schroeder, M. D., Long, F., Yang, J. S., He, Y., Ding, P., Kao, J. C., Wu, G. Y., Peng, H., Myers, G., & Lee, T. (2013). Clonal development and organization of the adult Drosophila central brain. *Curr Biol*, *23*(8), 633-643. https://doi.org/10.1016/j.cub.2013.02.057

Zhai, R. G., & Bellen, H. J. (2004). The architecture of the active zone in the presynaptic nerve terminal. *Physiology*, *19*(5), 262-270.

Zhang, F., Mak, S. O. K., Liu, Y., Ke, Y., Rao, F., Yung, W. H., Zhang, L., & Chow, B. K. C. (2022). Secretin receptor deletion in the subfornical organ attenuates the activation of excitatory neurons under dehydration. *Curr Biol*, *32*(22), 4832-4841 e4835. https://doi.org/10.1016/j.cub.2022.09.037

Zhang, L., Guo, X., & Zhang, W. (2022). Nutrients and pheromones promote insulin release to inhibit courtship drive. *Science Advances*, *8*(10), eabl6121.

Zheng, Z., Lauritzen, J. S., Perlman, E., Robinson, C. G., Nichols, M., Milkie, D., Torrens, O., Price, J., Fisher, C. B., Sharifi, N., Calle-Schuler, S. A., Kmecova, L., Ali, I. J., Karsh, B., Trautman, E. T., Bogovic, J. A., Hanslovsky, P., Jefferis, G., Kazhdan, M., . . . Bock, D. D. (2018). A Complete Electron Microscopy Volume of the Brain of Adult Drosophila melanogaster. *Cell*, *174*(3), 730-743 e722. https://doi.org/10.1016/j.cell.2018.06.019

Zimmerman, C. A., Leib, D. E., & Knight, Z. A. (2017). Neural circuits underlying thirst and fluid homeostasis. *Nature Reviews Neuroscience*, *18*(8), 459-469.

TABLES

Table S1: ISN postsynaptic partners

	Cell type / Classification	Flywire ID	Synapses from ISN 720575940619731393	Synapses from ISN 720575940628363855	Synapses from ISN 720575940625627932	Synapses from ISN 720575940624153528	Total synapses from 4 ISNs	Total synapses per cell type	Tracing contributions (number of edits)
1	FLAa2	720575940627559623	19	20	29	25	93		Jefferis Lab: Irene Salgarella (3), Varun Sane (1).
2	FLAa2	720575940613754833	19	32	21	19	91		Murthy and Seung Labs: James Hebditch (1), Ben Silverman (1), remer tancontian (1). Jefferis Lab: Bhargavi Parmar (4).

3	FLAa2	720575940621782057	18	14	21	7	60		Murthy and Seung Labs: Nash Hadjerol (6).
4	FLAa2	720575940623605180	10	10	14	14	48		Dickson Lab: Alisa Poh (1). Murthy and Seung Labs: Austin T Burke (16), Shirleyjoy Serona (1).
5	FLAa2	720575940625218590	7	16	11	10	44		Jefferis Lab: Irene Salgarella (8), Arti Yadav (1).
6	FLAa2	720575940620994292	7		23	14	44		Jefferis Lab: Irene Salgarella (1), Greg Jefferis (1), Philipp Schlegel (1), Bhargavi Parmar (1). Murthy and Seung Labs: Ben Silverman (1), Kendrick Joules Vinson (15), Joshua Bañez (2).
7	FLAa2	720575940632134483	17	6	13	6	42		Jefferis Lab: Imaan Tamimi (1), Arti Yadav (1). Murthy and Seung Labs: James Hebditch (2), Nash Hadjerol (1).
8	FLAa2	720575940619283553	11	10	9	12	42		Jefferis Lab: Arti Yadav (1). Murthy and Seung Labs: Austin T Burke (14).
9	FLAa2	720575940620306300	21		5	12	38		Murthy and Seung Labs: Austin T Burke (1), James Hebditch (2). Jefferis Lab: Arti Yadav (1).
10	FLAa2	720575940611991830	15	11	5		31		Jefferis Lab: Irene Salgarella (2). Murthy and Seung Labs: Austin T Burke (11).
11	FLAa2	720575940626512881	7		14	10	31		Murthy and Seung Labs: Mendell Lopez (10).
12	FLAa2	720575940621680264	8		10	16	34		Jefferis Lab: Anjali Pandey (1). Murthy and Seung Labs: Austin T Burke (12), J. Anthony Ocho (3).
13	FLAa2	720575940637381466	11	5		12	28		Jefferis Lab: Irene Salgarella (4). Murthy and Seung Labs: Zairene Lenizo (1).
14	FLAa2	720575940632695904	6	11	10		27		Jefferis Lab: Irene Salgarella (4), Rashmita Rana (1).
15	FLAa2	720575940631570636		6	14	6	26		Murthy and Seung Labs: Austin T Burke (5), Shirleyjoy Serona (3), Mendell Lopez (45).
16	FLAa2	720575940621605964	6		12	8	26		Seung Lab: Zhihao Zheng (1). Jefferis Lab: Irene Salgarella (9), Márcia Santos (2).
17	FLAa2	720575940637151807	8	5	13		26		Seung Lab: Zhihao Zheng (4). Jefferis Lab: A. Javier (2), Dickson Lab: Alisa Poh (3). Murthy and Seung Labs: James Hebditch (2), regine salem (1).
18	FLAa2	720575940622161032	15	9			24		Jefferis Lab: Irene Salgarella (4). Murthy and Seung Labs: Nash Hadjerol (8), Joshua Bañez (14).
19	FLAa2	720575940612087922	6		12	6	24		Jefferis Lab: Irene Salgarella (5). Murthy and Seung Labs: Austin T Burke (2), Nash Hadjerol (5).
20	FLAa2	720575940623752741	12	5	5		22		Jefferis Lab: Irene Salgarella (5).
21	FLAa2	720575940643191575		6	15		21		Murthy and Seung Labs: Mendell Lopez (11). Jefferis Lab: Arti Yadav (1).
22	FLAa2	720575940635191438		12		8	20		Jefferis Lab: Irene Salgarella (3). Murthy and Seung Labs: Zairene Lenizo (2).
23	FLAa2	720575940610624206	8		12		20		Jefferis Lab: Irene Salgarella (4). Murthy and Seung Labs: remer tancontian (2), J. Dolorosa (1).
24	FLAa2	720575940644751651	6	6	6		18		Jefferis Lab: Arti Yadav (1). Murthy and Seung Labs: Doug Bland (19).
25	FLAa2	720575940623989245		7		7	14		Jefferis Lab: Irene Salgarella (5). Murthy and Seung Labs: remer tancontian(1), Austin T Burke (1), Ben Silverman (2).
26	FLAa2	720575940623231527			9	5	14		Jefferis Lab: Yijie Yin (3). Dickson Lab: Alisa Poh (1). Murthy and Seung Labs: James Hebditch (1), Mendell Lopez (6).
27	FLAa2	720575940604764862	7		6		13		Jefferis Lab: Irene Salgarella (2). Murthy and Seung Labs: Mendell Lopez (1).
28	FLAa2	720575940628857850			13		13		Wolf Lab: fred wolf (1). Jefferis Lab: Arti Yadav (1), Yijie Yin (4). Murthy and Seung Labs: Mendell Lopez (3), remer tancontian (1).
29	FLAa2	720575940638900469	6		6		12		Jefferis Lab: Irene Salgarella (4).

30	FLAa2	720575940619398872	12				12		Jefferis Lab: A. Javier (1), Chitra Nair (1). Dickson Lab: Alisa Poh (13). Murthy and Seung Labs: Zairene Lenizo (4).
31	FLAa2	720575940631044141	6		6		12		Murthy and Seung Labs: James Hebditch (2). Jefferis Lab: Arti Yadav (1).
32	FLAa2	720575940638996413		5	7		12		Dickson Lab: Alisa Poh (8). Murthy and Seung Labs: Kyle Patrick Willie (2), Shirleyjoy Serona (3), Kendrick Joules Vinson (1), Joshua Bañez (1), James Hebditch (1). Jefferis Lab: Arti Yadav (1), Bhargavi Parmar (1).
33	FLAa2	720575940624735565	6		5		11		Dickson Lab: Alisa Poh (1). Jefferis Lab: Varun Sane (1), Arti Yadav (1). Murthy and Seung Labs: Ryan Willie (24), Rey Adrian Candilada (1).
34	FLAa2	720575940622266748		5		5	10		Jefferis Lab: Rashmita Rana (1), Zeba Vohra (1). Murthy and Seung Labs: Shirleyjoy Serona (15).
35	FLAa2	720575940644327022		5	5		10		Murthy and Seung Labs: James Hebditch (2). Jefferis Lab: Arti Yadav (1). Murthy and Seung Labs: J. Dolorosa (7).
36	FLAa2	720575940637002724	8				8		Jefferis Lab: Imaan Tamimi (1), Irene Salgarella (5). Murthy and Seung Labs: Darrel Jay Akiatan (2), J. Anthony Ocho (18).
37	FLAa2	720575940612348438				8	8		Jefferis Lab: Anjali Pandey (1). Murthy and Seung Labs: Zairene Lenizo (2), Kendrick Joules Vinson (4), Rey Adrian Candilada (3).
38	FLAa2	720575940623063847	8				8		Jefferis Lab: Arti Yadav (1). Murthy and Seung Labs: Shirleyjoy Serona (17).
39	FLAa2	720575940616872337		7			7		Jefferis Lab: Rashmita Rana (1). Murthy and Seung Labs: Ben Silverman (8), Kendrick Joules Vinson (6), Kyle Patrick Willie (1).
40	FLAa2	720575940626982165		6			6		Seung Lab: Zhihao Zheng (4). Jefferis Lab: Irene Salgarella (4), Yijie Yin (2). Murthy and Seung Labs: Nash Hadjerol (8).
41	FLAa2	720575940619403435		5			5		Jefferis Lab: Marta Costa (3), Irene Salgarella (1), Anjali Pandey (1), Varun Sane (18).
42	FLAa2	720575940626742532			5		5		Jefferis Lab: Marta Costa (3), Irene Salgarella (1), Anjali Pandey (1), Varun Sane (18).
43	FLAa2	720575940630393427			5		5		Jefferis Lab: Irene Salgarella (9).
44	FLAa2	720575940616510425		5			5		Dickson Lab: Alisa Poh (5). Murthy and Seung Labs: Rey Adrian Candilada (1).
45	FLAa2	720575940634776511			5		5		Jefferis Lab: Imaan Tamimi (2), Arti Yadav (1). Dickson Lab: Alisa Poh (2). Murthy and Seung Labs: Mendell Lopez (8), Ariel Dagohoy (19), Joshua Bañez (2), Ben Silverman (1).
46	FLAa2	720575940605589378				5	5	1080	Jefferis Lab: Arti Yadav (1). Murthy and Seung Labs: Austin T Burke (15), Zairene Lenizo (1).
47	Handshake	720575940651601910	54	51	51	35	191		Jefferis and Waddell Labs: Joseph Hsu (1). Wolf Lab: fred wolf (1). Scott Lab: Amanda Abusaif (2). Murthy and Seung Labs: Ariel Dagohoy (2), J. Anthony Ocho (2), Shirleyjoy Serona (13). Jefferis Lab: Sangeeta Sisodiya (23).
48	Handshake	720575940626449158	46	46	42	37	171		Jefferis and Waddell Labs: Joseph Hsu (1). Scott Lab: Amanda Abusaif (1).
49	Handshake	720575940618791515	45	51	49	38	183		Wolf Lab: fred wolf (2). Scott Lab: Amanda Abusaif (3).
50	Handshake	720575940622839786	39	56	44	38	177	722	Jefferis and Waddell Labs: Joseph Hsu (1). Jefferis Lab: Laia Serratosa (1), Rashmita Rana (1). Dickson Lab: Alisa Poh (1). Murthy and Seung Labs: Kyle Patrick Willie (4), remer tancontian (5), Austin T Burke (8). Itisha Joshi (15).
51	Cowboy L fragment	720575940611730674	72	95	75	59	301		Simpson Lab: Li Guo (7). Jefferis Lab: Yijie Yin (2), Siqi Fang (3). Scott Lab: Amanda González-Segarra (7), Amanda Abusaif (1). Murthy and Seung Labs: J. Anthony Ocho (2), Mendell Lopez (1), Shaina Mae Monungolh (7), Ben Silverman (1), Nash Hadjerol (1), remer tancontian (1), Miguel Albero (2), Rey Adrian Candilada (2).
52	Cowboy R	720575940624514492	36	51	38	34	159	460	Jefferis and Wilson Labs: Laia Serratosa Capdevila (6). Jefferis Lab: Yijie Yin (6), Katharina Eichler (2), Zeba Vohra (18). Scott Lab: Amanda Abusaif (6). Murthy and Seung Labs: J. Dolorosa (1), Austin T Burke (10), Darrel Jay Akiatan (13)

53	SEZ: GNG.GNG. 2607	720575940633170969	37	30	33	24	124		Murthy and Seung Labs: Ryan Willie (32), Joshua Bañez (1), remer tancontian (1), Nash Hadjerol (1). Jefferis Lab: Katharina Eichler (1), Dhwani Patel (4), Griffin Badalemente (2), Dharini Sapkal (1).
54	SEZ: PRW.GNG. 9	720575940616167730	35	19	40	21	115		Jefferis Lab: Arti Yadav (1), Griffin Badalemente (2), Dharini Sapkal (5), Yashvi Patel (2), Bhargavi Parmar (1). Scott Lab: Amanda González-Segarra (3). Murthy and Seung Lab: Mendell Lopez (12).
55	SEZ: PRW.PRW .166	720575940622732253	5	12	17		34		Jefferis Lab: Rashmita Rana (1), Zeba Vohra (4). Murthy and Seung Labs: Shirleyjoy Serona (55), Austin T Burke (1). Kim Lab: Chan Hyuk Kang (1).
56	SEZ: PRW.PRW .214	720575940625178768	8	6		17	31		Jefferis Lab: Rashmita Rana (1), Sangeeta Sisodiya (1). Murthy and Seung Labs: Ben Silverman (7), Shirleyjoy Serona (23), Austin T Burke (1), Zairene Lenizo (4), Kyle Patrick Willie (2).
57	SEZ: PRW.GNG. 6	720575940614736290	8	8	5	5	26		Murthy and Seung Labs: Ryan Willie (1), Ben Silverman (1), J. Anthony Ocho (37), Nash Hadjerol (2). Jefferis Lab: Chitra Nair (1), Yashvi Patel (1).
58	SEZ: PRW.GNG. 12	720575940619042427			8		8		Seeds Hampel Lab: Patricia Pujols (7). Murthy and Seung Labs: Zairene Lenizo (4), Rey Adrian Candilada (1), remer tancontian (1), Kendrick Joules Vinson (1). Jefferis Lab: Bhargavi Parmar (5).
59	SEZ: PRW.PRW .146	720575940621490721				6	6		Jefferis Lab: Arti Yadav (1). Murthy and Seung Labs: J. Anthony Ocho (2), Ben Silverman (3), Shaina Mae Monungolh (1), Kyle Patrick Willie (4).
60	SEZ: GNG.GNG. 1075	720575940620627803	5				5		Jefferis Lab: Shanice Bailey (3), Rashmita Rana (1), Dhwani Patel (1). Murthy and Seung Labs: J. Anthony Ocho (1).
61	SEZ: PRW.PRW .42	720575940613120721			5		5		Murthy and Seung Labs: Nash Hadjerol (9). Kim Lab: hanetwo (1).
62	SEZ: PRW.PRW .62	720575940615052812			5		5		Jefferis Lab: Arti Yadav (1). Murthy and Seung Labs: Austin T Burke (1), Zairene Lenizo (2), Rey Adrian Candilada (1), Szi-chieh Yu (1). Jefferis Lab: Dharini Sapkal (1).
63	SEZ: PRW.PRW .199	720575940624532408			5		5		Jefferis Lab: Arti Yadav (1). Murthy and Seung Labs: Jay Gager (9). Itisha Joshi (2).
64	SEZ: FLA_L.FLA _L.47	720575940631299602			5		5		Jefferis Lab: Katharina Eichler (10), Laia Serratosa (1), Marina Gkantia (11), Bhargavi Parmar (28), Dharini Sapkal (10). Murthy and Seung Labs: J. Anthony Ocho (1), Zairene Lenizo (4), Shirleyjoy Serona (41), Darrel Jay Akiatan (1). Scott Lab: Amanda Abusaif (2). Itisha Joshi (5).
65	SEZ: PRW.PRW .120	720575940619866059			5		5		Jefferis Lab: Yijie Yin (1), Rashmita Rana (1), Zeba Vohra (10). Murthy and Seung Labs: Michelle Pantujan (1), Zairene Lenizo (1), regine salem (88), Rey Adrian Candilada (1), remer tancontian (3)
66	SEZ: TRdm	720575940612921571			5		5	379	Murthy and Seung Labs: Doug Bland (5). Jefferis Lab: Imaan Tamimi (1), Laia Serratosa (1), Griffin Badalemente (1), Dhwani Patel (15).
67	DSOG 1	720575940617291323	32	33	36	22	123		Seeds Hampel Lab: Katharina Eichler (10). Jefferis and Wilson Labs: Laia Serratosa Capdevila (2). Jefferis Lab: A. Javier (8), Katharina Eichler (1), Yijie Yin (1), Dharini Sapkal (47), Arzoo Diwan (6), Dhara Kakadiya (7), Zeba Vohra (9), Dhwani Patel (10), Yashvi Patel (1). Scott Lab: Amanda Abusaif (21). Pankratz Lab: Damian Demarest (1). Murthy and Seung Labs: remer tancontian (6), J. Dolorosa (54), Kendrick Joules Vinson (3), Shaina Mae Monungolh (2), Zairene Lenizo (2). Itisha Joshi (5)
68	DSOG 1	720575940623529610	28	27	32	31	118		Seeds Hampel Lab: Katharina Eichler (3). Jefferis and Wilson Labs: Laia Serratosa Capdevila (8). Jefferis Lab: Irene Salgarella (3), Yijie Yin (2), Zeba Vohra (7), Arti Yadav (16), Bhargavi Parmar (25), Chitra Nair (39), Dhara Kakadiya (4). Scott Lab: Amanda Abusaif (12). Murthy and Seung Labs: Celia D (1), remer tancontian (2), Austin T Burke (4), Zairene Lenizo (11), Shaina Mae Monungolh (26), Rey Adrian Candilada (1), Shirleyjoy Serona (24), J. Anthony Ocho (3). Itisha Joshi (6)

69	DSOG 1	720575940623338281	19	14	8	8	49		Seeds Hampel Lab: Katharina Eichler (8). Jefferis Lab: Siqi Fang (14), Katharina Eichler (4), Irene Salgarella (2), Griffin Badalemente (7), Nidhi Patel (3), Zeba Vohra (15), Dhwani Patel (10), Chitra Nair (8), Yashvi Patel (15), Dharini Sapkal (19), Arti Yadav (4). Murthy and Seung Labs: Rey Adrian Candilada (6), Shaina Mae Monungolh (45). Kim Lab: Chan Hyuk Kang (2). Scott Lab: Amanda Abusaif (12).
70	DSOG 1	720575940644666660	13	5	17	5	40	330	Seeds Hampel Lab: Katharina Eichler, Steven Calle, Lucia Kmecova, Alexis E Santana Cruz. Murthy and Seung Labs: remer tancontian, Zairene Lenizo.
71	SEZ & SMP: FLA_L.SMP_L.27	720575940626500362	19	5	18	8	50		Jefferis Lab: Greg Jefferis (2). Dickson Lab: Alisa Poh (1). Murthy and Seung Labs: Shirleyjoy Serona (25), regine salem (17), Mendell Lopez (1), Shaina Mae Monungolh (2).
72	SEZ & SMP: VESa1	720575940632951597	12		19	16	47		Murthy and Seung Labs: Austin T Burke (72), Sarah Morejohn (1), Kyle Patrick Willie (11), James Hebditch (6), Doug Bland (5), Nash Hadjerol (39), Ben Silverman (7), J. Dolorosa (3), Zairene Lenizo (48), Mendell Lopez (9), Shaina Mae Monungolh (5), Rey Adrian Candilada (7), regine salem (80), remer tancontian (19), Darrel Jay Akiatan (13), Joshua Bañez (112), Ariel Dagohoy (9), Kendrick Joules Vinson (27), Miguel Albero (4), Shirleyjoy Serona (89), Michelle Pantujan (14), J. Anthony Ocho (11). Jefferis and Wilson Labs: Laia Serratosa Capdevila (6). Jefferis Lab: Marlon Blanquart (1), Imaan Tamimi (5), Yijie Yin (3), Irene Salgarella (3), Varun Sane (4), Griffin Badalemente (21), Philipp Schlegel (9), Dharini Sapkal (35), Chitra Nair (34), Arzoo Diwan (8), Zeba Vohra (24), Anjali Pandey (2), Dhara Kakadiya (48), Bhargavi Parmar (10), Kaushik Parmar (1), Arti Yadav (10), Yashvi Patel (12), Greg Jefferis (1). Janelia Tracers: Tansy Yang (38). Selcho Lab: Mareike Selcho (1).
73	SEZ & SMP: FLA_L.SMP_L.32	720575940627436554	12	16	6	12	46		Jefferis Lab: Greg Jefferis (1), Christophe Dunne (1), Bhargavi Parmar (1). Murthy and Seung Labs: Mendell Lopez (1), Joshua Bañez (2).
74	SEZ & SMP: FLA_R.SMP_R.32	720575940645920052	7		17	13	37		Jefferis and Wilson Labs: Laia Serratosa Capdevila (1). Wolf Lab: fred wolf (1). Huetteroth Lab: Wolf Huetteroth (1). Murthy and Seung Labs: Zairene Lenizo (6), Shirleyjoy Serona (29), Ariel Dagohoy (28), Shaina Mae Monungolh (11). Jefferis Lab: Márcia Santos (1).
75	SEZ & SMP: BiT2	720575940621662332	7	7	14	8	36		Murthy and Seung Labs: Austin T Burke (47), Joshua Bañez (9), Kyle Patrick Willie (16). Jefferis Lab: Imaan Tamimi (12), Yijie Yin (2), Bhargavi Parmar (2), Dharini Sapkal (1). Scott Lab: Amanda Abusaif (14).
76	SEZ & SMP: FLA_R.SMP_R.30	720575940637780969	5	5	10	14	34		Jefferis Lab: Arti Yadav (1), Dhwani Patel (5). Murthy and Seung Labs: Shirleyjoy Serona (3), Ryan Willie (2), Kyle Patrick Willie (2), Rey Adrian Candilada (1).
77	SEZ & SMP: Lgr3/FLAa3	720575940626452879	8	15	9		32		Jefferis Lab: Yijie Yin (1), Anjali Pandey (1). Murthy and Seung Labs: James Hebditch (1), Mendell Lopez (21), Austin T Burke (3), Joshua Bañez (3), Kendrick Joules Vinson (4).
78	SEZ & SMP: SMPpv2	720575940623701768		6	9		15		Jefferis Lab: Greg Jefferis (1), Yijie Yin (2), A. Javier (3), Irene Salgarella (5). Scott Lab: Amanda Abusaif (1). Murthy and Seung Labs: Szi-chieh Yu (15), Zairene Lenizo (9).
79	SEZ & SMP: SMPpv2	720575940628310275		7		5	12		Jefferis and Wilson Labs: Laia Serratosa Capdevila (9). Jefferis Lab: Katharina Eichler (9), Imaan Tamimi (5), Irene Salgarella (4), Philipp Schlegel (39). Murthy and Seung Labs: James Hebditch (1), Rey Adrian Candilada (10).
80	SEZ & SMP: Lgr3/FLAa3	720575940629764906		5			5		Jefferis and Waddell Labs: Joseph Hsu (3). Murthy and Seung Labs: Austin T Burke (14). Jefferis Lab: Anjali Pandey (1).
81	SEZ & SMP: Gallinule	720575940618926757				5	5	319	Jefferis and Waddell Labs: Joseph Hsu (8). Jefferis Lab: Yijie Yin (4), Imaan Tamimi (1), Rashmita Rana (2). Murthy and Seung Labs: Mendell Lopez (2).
82	BiT	720575940610708430	71	74	93	63	301	301	Jefferis Lab: Yijie Yin (3), A. Javier (1), Imaan Tamimi (22), Varun Sane (2), Griffin Badalemente (1), Dhara Kakadiya (1), Arti Yadav (6). Murthy and Seung Labs: Claire McKellar (1), Michelle Pantujan (2), Austin T Burke (2), James Hebditch (1), J. Anthony Ocho (420), Rey Adrian Candilada (1), Nash Hadjerol (4). Wes Murfin (1). Scott Lab: Amanda Abusaif (30).

83	Ascending neuron: FLA_R.PRW.5	720575940625841241	20	6	16	27	69		Seeds Hampel Lab: Steven Calle (1). Jefferis Lab: Katharina Eichler (8). Kim Lab: Chan Hyuk Kang (2). Murthy and Seung Labs: M Sorek (2), J. Anthony Ocho (1), Zairene Lenizo (1).
84	Ascending neurons: PRW.FLA_L.15	720575940633548128		29	33	5	67		Jefferis and Wilson Labs: Laia Serratosa Capdevila (11). Scott Lab: Zepeng Yao (1), Amanda Abusaif (2), Amanda González-Segarra (5), Rey Adrian Candilada (4).
85	Ascending neuron: FLA_L.FLA_L.25	720575940621599741	19	18		5	42		Jefferis and Waddell Labs: Joseph Hsu (3). Jefferis and Wilson Labs: Laia Serratosa Capdevila (3).
86	Ascending neuron: PRW.SMP_L.30	720575940635527092	8	5	14	11	38		Seeds Hampel Lab: Katharina Eichler (27). Jefferis and Wilson Labs: Laia Serratosa Capdevila (15). Jefferis Lab: Katharina Eichler (1), Varun Sane (1), Irene Salgarella (1), Bhargavi Parmar (10), Chitra Nair (40), Sangeeta Sisodiya (18), Zeba Vohra (4), Bhargavi Parmar (10), Dharini Sapkal (1). Murthy and Seung Labs: Zairene Lenizo (5), J. Anthony Ocho (3), Nash Hadjerol (5), Mendell Lopez (3), Joshua Bañez (4), regine salem (1), Rey Adrian Candilada (1), Kendrick Joules Vinson (3), Ariel Dagohoy (8), Kyle Patrick Willie (4), Doug Bland (31), Ryan Willie (1). Itisha Joshi (25)
87	Ascending neuron: FLA_R.PRW.2	720575940611548273	10	11	5		26		Jefferis and Wilson Labs: Laia Serratosa Capdevila (11). Murthy and Seung Labs: Mendell Lopez (1), Zairene Lenizo (2), Kyle Patrick Willie (4).
88	Ascending neuron: PRW.PRW.304	720575940631295506	7		9		16		Jefferis and Wilson Labs: Laia Serratosa Capdevila (3). Murthy and Seung Labs: Shaina Mae Monungolh (2), Nash Hadjerol (7). Jefferis Lab: Dhwani Patel (1).
89	Ascending neuron: PRW.PRW.343	720575940636263543	5		8		13		Seung Lab: Zhihao Zheng (1). Jefferis Lab: Katharina Eichler (1), Dharini Sapkal (5). Murthy and Seung Labs: Michelle Pantujan (2), Nash Hadjerol (7), Shaina Mae Monungolh (1). Dickson Lab: Alisa Poh (2).
90	Ascending neuron: PRW.PRW.137	720575940620833901			6	6	12		Murthy and Seung Labs: James Hebditch (9), Austin T Burke (11), Ben Silverman (1), Nash Hadjerol (3), Mendell Lopez (18), Ryan Willie (1), regine salem (3), Joshua Bañez (6), Rey Adrian Candilada (5), Zairene Lenizo (7), Darrel Jay Akiatan (3). Jefferis and Wilson Labs: Laia Serratosa Capdevila (3). Jefferis Lab: Katharina Eichler (10), Sangeeta Sisodiya (1), Dharini Sapkal (1), Bhargavi Parmar (37), Chitra Nair (17). Seeds Hampel Lab: Alexis E Santana Cruz (1).
91	Ascending neuron: PRW.PRW.247	720575940627304424				10	10		Jefferis Lab: Dharini Sapkal (1). Murthy and Seung Labs: Shirleyjoy Serona (16), Zairene Lenizo (1), Rey Adrian Candilada (3).
92	Ascending neuron: FLA_L.GNG.5	720575940617662950			6		6	299	Jefferis Lab: Katharina Eichler. Murthy and Seung Labs: Ben Silverman.
93	Descending neuron: PRW.GNG.16	720575940621328048	7	16	15	9	47		Jefferis and Wilson Labs: Laia Serratosa Capdevila (3). Jefferis Lab: Katharina Eichler (1), Arti Yadav (1), Dharini Sapkal (1), Dhwani Patel (1), Bhargavi Parmar (31). Murthy and Seung Labs: Austin T Burke (1), Mendell Lopez (1), Shaina Mae Monungolh (7), Ariel Dagohoy (1). Itisha Joshi (5).
94	Descending neuron: FLA_L.GNG.3	720575940610610841	9			5	14		Jefferis and Wilson Labs: Laia Serratosa Capdevila (14). Jefferis Lab: A. Javier (9), Yijie Yin (3), Katharina Eichler (1), Rashmita Rana (1).
95	Descending neuron: FLA_L.NO_OUT.7	720575940625587325	7		5		12		Jefferis Lab: Philipp Schlegel (1), Katharina Eichler (15), Paul Brooks (45). Jefferis and Wilson Labs: Laia Serratosa Capdevila (3). Selcho Lab: Mareike Selcho (7). Kim Lab: Usb (1).
96	Descending neuron: GNG.GNG.1079	720575940620668609			12		12		Seeds Hampel Lab: Katharina Eichler (2), Stefanie Hampel (1). Jefferis and Wilson Labs: Laia Serratosa Capdevila (1). Jefferis Lab: Griffin Badalemente (1), Dhwani Patel (30), Dharini Sapkal (18). Murthy and Seung Labs: regine salem (1).

97	Descending Neuron: Gumdrop	720575940630697078	5			6	11		Jefferis and Wilson Labs: Laia Serratosa Capdevila (21). Jefferis Lab: Katharina Eichler (30), Imaan Tamimi (1), Yashvi Patel (5), Arti Yadav (10), Zeba Vohra (23), Bhargavi Parmar (15). Murthy and Seung Labs: Nash Hadjerol (5). Itisha Joshi (8).
98	Descending neuron: FLA_L.NO_OUT.5	720575940619576001	6		5		11		Jefferis and Wilson Labs: Laia Serratosa Capdevila (3). Jefferis Lab: Katharina Eichler (17), Paul Brooks (28), Imaan Tamimi (1), Yijie Yin (8). Murthy and Seung Labs: Michelle Pantujan (1), J. Dolorosa (1), Ben Silverman (14).
99	Descending neuron	720575940644812398		6	5		11		Jefferis and Wilson Labs: Laia Serratosa Capdevila (4). Jefferis Lab: A. Javier (24), Katharina Eichler (4), Rashmita Rana (1), Varun Sane (1). Selcho Lab: Mareike Selcho (8). Murthy and Seung Labs: Joshua Bañez (1).
100	Descending neuron: GNG.GNG.391	720575940612692889	6				6	124	Jefferis and Wilson Labs: Laia Serratosa Capdevila (2). Jefferis Lab: Katharina Eichler (2), Zeba Vohra (1), Yashvi Patel (2). Murthy and Seung Labs: Shirleyjoy Serona (253), Darrel Jay Akiatan (5).
101	ISN	720575940625627932	5	6		5	16		Scott Lab: Alexander Edward Del Toro BSc (1). Jefferis Lab: Arti Yadav (1). Kim Lab: Hyungjun Choi (183), Chan Hyuk Kang (26), hanetwo (5). Murthy and Seung Labs: Ariel Dagohoy (2), Rey Adrian Candilada (3).
102	ISN	720575940619731393		5		5	10		Jefferis Lab: Katharina Eichler (1). Murthy and Seung Labs: Claire McKellar (1), Nash Hadjerol (2), Celia D (1), regine salem (332), Joshua Bañez (286), Kendrick Joules Vinson (8), J. Anthony Ocho (1). Scott Lab: Amanda González-Segarra (3), Alexander Edward Del Toro BSc (1). Kim Lab: Keehyun Park (6), hanetwo (19).
103	ISN	720575940628363855			5		5		Kim Group: Hyungjun Choi (29), Chan Hyuk Kang (25), hanetwo (3). Murthy and Seung Labs: Shaina Mae Monungolh (5), Joshua Bañez (1), Shirleyjoy Serona (126), Zairene Lenizo (1).
104	ISN	720575940624153528			5		5	20	Scott Lab: Amanda González-Segarra (1). Jefferis Lab: Anjali Pandey (1), Varun Sane (1). Kim Lab: Keehyun Park (1), hanetwo (22). Murthy and Seung Labs: Nash Hadjerol (12), Zairene Lenizo (4), remer tancontian (1).
								4034	

Table S2: BiT postsynaptic neurons

	Name	Neuron ID	Synapses from BiT	Total synapses from BiT per cell type	Tracing contributions (number of edits)
1	IPC	720575940650527222	54		Jefferis Lab: Imaan Tamimi (2), Anjali Pandey (1). Murthy and Seung Labs: Austin T Burke (4).
2	IPC	720575940603765280	44		Maimon Lab: Gaby Maimon (1). Jefferis Lab: Katharina Eichler (2). Murthy and Seung Labs: Austin T Burke (3).
3	IPC	720575940620932045	39		Jefferis Lab: Imaan Tamimi (2), Laia Serratosa (7). Murthy and Seung Labs: Austin T Burke (6).
4	IPC	720575940612923390	33		Jefferis Lab: Imaan Tamimi (1), Laia Serratosa (6), Markus Pleijzier (1), Rashmita Rana (1). Murthy and Seung Labs: Ryan Willie (1).
5	IPC	720575940625379859	30		Jefferis Lab: A. Javier (4), Irene Salgarella (2), Laia Serratosa (9). Murthy and Seung Labs: Austin T Burke (4).

6	IPC	720575940622897639	28		Seung Lab: Zhihao Zheng (1), Jefferis Lab: A. Javier (1). Dacks Lab: Andrew Dacks (1). Murthy and Seung Labs: Austin T Burke (7).
7	IPC	720575940643539566	26		Jefferis Lab: Imaan Tamimi (3), A. Javier (7), Laia Serratosa (4), Rashmita Rana (1). Murthy and Seung Labs: Austin T Burke (13).
8	IPC	720575940620628957	25		Jefferis Lab: Imaan Tamimi (1), A. Javier (6). Murthy and Seung Labs: Austin T Burke. (18)
9	IPC	720575940623081400	22		Jefferis Lab: Markus Pleijzier (5). Murthy and Seung Labs: Austin T Burke (18).
10	IPC	720575940631884883	22		Dacks Lab: Andrew Dacks (1). Jefferis Lab: Imaan Tamimi (1), Laia Serratosa (8). Murthy and Seung Labs: Austin T Burke (7). Itisha Joshi (2).
11	IPC	720575940628363820	22		Jefferis Lab: Imaan Tamimi (1). Dacks Lab: Andrew Dacks (1). Murthy and Seung Labs: Austin T Burke (6). Scott Lab: Meghan Laturney (1).
12	IPC	720575940624064295	22		Dacks Lab: Andrew Dacks (1). Jefferis Lab: Imaan Tamimi (3), Laia Serratosa (10), Anjali Pandey (1). Murthy and Seung Labs: Austin T Burke (5).
13	IPC	720575940628199802	21		Jefferis Lab: Markus Pleijzier (1), A. Javier (1), Laia Serratosa (9), Philipp Schlegel (1). Murthy and Seung Labs: Austin T Burke (1). Wolf Lab: Fred Wolf (1).
14	IPC	720575940623586284	17		Jefferis Lab: Imaan Tamimi (1), Márcia Santos (4). Murthy and Seung Labs: Austin T Burke (66).
15	IPC	720575940618694827	14		Jefferis Lab: A. Javier (3), Imaan Tamimi (1), Laia Serratosa (12), Anjali Pandey (1).
16	IPC	720575940614623455	10		Murthy and Seung Labs: James Hebditch (4), Nash Hadjerol (1), Doug Bland (6), Joshua Bañez (6). Jefferis Lab: Philipp Schlegel (1).
17	IPC	720575940611254681	7		Jefferis Lab: Markus Pleijzier (2), A. Javier (3), Imaan Tamimi (9). Murthy and Seung Labs: Austin T Burke (13). Kim Lab: Minsik Yun (2).
18	IPC	720575940615911380	6	442	Jefferis Lab: A. Javier (6), Laia Serratosa (6), Philipp Schlegel (1). Murthy and Seung Labs: Ryan Willie (1).
19	Lgr3/FLAa3	720575940626983185	36		Jefferis Lab: Irene Salgarella (10). Murthy and Seung Labs: James Hebditch (5), Kyle Patrick Willie (4), Rey Adrian Candilada (1), Kendrick Joules Vinson (11), Zairene Lenizo (2), Nash Hadjerol (4).
20	Lgr3/FLAa3	720575940620201084	32		Jefferis Lab: Irene Salgarella (7), Laia Serratosa (4). Murthy and Seung Labs: James Hebditch (4).
21	Lgr3/FLAa3	720575940613895934	31		Jefferis Lab: Irene Salgarella (10), Dharini Sapkal (2), Dhwani Patel (12). Murthy and Seung Labs: James Hebditch (2), Zairene Lenizo (2), Joshua Bañez (8).
22	Lgr3/FLAa3	720575940629696763	30		Jefferis Lab: Anjali Pandey (1). Murthy and Seung Labs: James Hebditch (4), Nash Hadjerol (6), Ben Silverman (1), Darrel Jay Akiatan (2).
23	Lgr3/FLAa3	720575940644053271	19		Jefferis Lab: Anjali Pandey (1), Christopher Dunne (11). Murthy and Seung Labs: Zairene Lenizo (1).
24	Lgr3/FLAa3	720575940630329903	19		Jefferis Lab: Irene Salgarella (15). Murthy and Seung Labs: James Hebditch (3).
25	Lgr3/FLAa3	720575940616987426	19		Murthy and Seung Labs: James Hebditch (4). Jefferis Lab: Anjali Pandey (8), Christopher Dunne (4), Sangeeta Sisodiya (1), Dharini Sapkal (4).
26	Lgr3/FLAa3	720575940639420032	19		Jefferis Lab: Irene Salgarella (16). Murthy and Seung Labs: James Hebditch (4), Zairene Lenizo (1).
27	Lgr3/FLAa3	720575940614714299	18		Jefferis Lab: Irene Salgarella (7). Murthy and Seung Labs: Nash Hadjerol (1).
28	Lgr3/FLAa3	720575940632879842	18		Scott Lab: Zepeng Yao (17). Jefferis Lab: Arti Yadav (1), Bhargavi Parmar (6). Murthy and Seung Labs: J. Anthony Ocho (1), Austin T Burke (1), Zairene Lenizo (2).
29	Lgr3/FLAa3	720575940626179658	15		Jefferis Lab: Irene Salgarella (10).
30	Lgr3/FLAa3	720575940626327070	15	271	Murthy and Seung Labs: Austin T Burke (1), James Hebditch (4), Ariel Dagohoy (4), Nash Hadjerol (2). Janelia tracers: Tansy Yang (2). Jefferis Lab: Irene Salgarella (8), Laia Serratosa (3). Scott Lab: Zepeng Yao (3). Pankratz Lab: Damian Demarest (2).
31	SMP & SLP: SMP_L.SMP_L.276	720575940617650203	45		Jefferis and Waddell Labs: Joseph Hsu (2). Murthy and Seung Labs: Kyle Patrick Willie (32). Jefferis Lab: Laia Serratosa (1), Anjali Pandey (1), Yijie Yin (4).

32	SMP & SLP: SMP_R.SMP_R.278	720575940619352198	44		Murthy Lab: Lucas Encarnacion-Rivera (1), Bock Lab: Davi Bock (4). Jefferis Lab: Yijie Yin (13), Greg Jefferis (15).
33	SMP & SLP: SMPpv1; right	720575940631373869	38		Jefferis and Waddell Labs: Joseph Hsu (2). Jefferis Lab: Irene Salgarella (1). Murthy and Seung Labs: J. Dolorosa (2), Kyle Patrick Willie (4).
34	SMP & SLP: SMPpv1; left	720575940633754292	26		Jefferis Lab: Yijie Yin (2). Murthy and Seung Labs: Ben Silverman (1).
35	SMP & SLP: SMP_R.SMP_R.808	720575940635354981	12		Murthy and Seung Labs: Zairene Lenizo (1), Nash Hadjerol (24), remer tancontian (5). Jefferis Lab: Anjali Pandey (1).
36	SMP & SLP: SMPpd1; left	720575940627327750	12		Jefferis Lab: Rashmita Rana (1). Murthy and Seung Labs: James Hebditch (3), remer tancontian (1).
37	SMP & SLP: SMP_R.SMP_R.70	720575940611332722	11		Jefferis Lab: Yijie Yin (1), Rashmita Rana (1). Murthy and Seung Labs: Kyle Patrick Willie (10.
38	SMP & SLP: SMPpd1; left	720575940619099558	10		Jefferis Lab: A. Javier (2), Arti Yadav (1).
39	SMP & SLP: SMP_R.SMP_R.742	720575940631589407	9		Murthy and Seung Labs: Austin T Burke (17), James Hebditch (2), Kendrick Joules Vinson (1). Jefferis Lab: Anjali Pandey (1).
40	SMP & SLP: SLPal1	720575940618140283	8		Jefferis Lab: A. Javier (3). Murthy and Seung Labs: Nash Hadjerol (1), Ariel Dagohoy (1), James Hebditch (2).
41	SMP & SLP: SMPpd2	720575940619949556	7		Jefferis Lab: Irene Salgarella (3), Anjali Pandey (1).
42	SMP & SLP: SMP_R.SMP_R.757	720575940632526547	6		Murthy and Seung Labs: Austin T Burke (1), Kyle Patrick Willie (6), Mendell Lopez (10), Doug Bland (24), remer tancontian (6). Jefferis Lab: Anjali Pandey (1).
43	SMP & SLP: SMP_L.SMP_L.706	720575940629298679	6		Murthy Lab: Lucas Encarnacion-Rivera (3). Jefferis Lab: A. Javier (1), Varun Sane (8), Arti Yadav (1). Murthy and Seung Labs: Kendrick Joules Vinson (7), remer tancontian (2).
44	SMP & SLP: SMP_R.SMP_R.906	720575940640456923	6		Jefferis Lab: Philipp Schlegel (3), Yijie Yin (1), Varun Sane (6), Anjali Pandey (1). Selcho Lab: Mareike Selcho (17). Murthy and Seung Labs: Mendell Lopez (19), Kyle Patrick Willie (1).
45	SMP & SLP: DM3; right	720575940621647498	5		Jefferis Lab: A. Javier (1), Yijie Yin (1).
46	SMP & SLP: DM3_canonical	720575940619899668	5		Jefferis Lab: Yijie Yin (16). Murthy and Seung Labs: Nash Hadjerol (1), Kyle Patrick Willie (1).
47	SMP & SLP: SMP_R.SMP_R.677	720575940629901307	5		Jefferis Lab: Yijie Yin (2), Chitra Nair (1), Varun Sane (3). Murthy and Seung Labs: Zairene Lenizo (2).
48	SMP & SLP: SLP_L.LH_L.5	720575940616707545	5		Jefferis and Wilson Labs: Laia Serratosa Capdevila (1). Wes Murfin (4). Jefferis Lab: Yijie Yin (3), Varun Sane (1), Dhara Kakadiya (2), Chitra Nair (4). Murthy and Seung Labs: Doug Bland (3), Kendrick Joules Vinson (23), Joshua Bañez (10), Rey Adrian Candilada (1).
49	SMP & SLP: SLP_R.SLP_R.557	720575940629163419	5		Murthy and Seung Labs: Austin T Burke (3). Jefferis Lab: Tomke S (14), Griffin Badalemente (4), Yijie Yin (1), Varun Sane (4), Dhwani Patel (1).
50	SMP & SLP: SMP_L.SMP_L.578	720575940626063688	5	270	Murthy and Seung Labs: Austin T Burke (13).
51	CCHa2R (RA)	720575940638190133	65		Murthy and Seung Labs: Claire McKellar (1). Jefferis Lab: Anjali Pandey (1), Laia Serratosa (117), Dhwani Patel (3). Scott Lab: Amanda Abusaif (1), Zepeng Yao (27). Kim Lab: hanetwo (1).
52	CCHa2R (RA)	720575940615181910	64		Jefferis Lab: Anjali Pandey (1). Scott Lab: Amanda Abusaif (12). Murthy and Seung Labs: Michelle Pantujan (41), Ryan Willie (459).
53	CCHa2R (RA)	720575940629642460	50		Jefferis and Waddell Labs: Joseph Hsu (1). Murthy and Seung Labs: Claire McKellar (12), Ryan Willie (1), Shirleyjoy Serona (1), Doug Bland (296), J. Anthony Ocho (3). Jefferis Lab: Arti Yadav (1). Kim Lab: Hyungjun Choi (74).
54	CCHa2R (RA)	720575940611411162	49	228	Murthy and Seung Labs: Claire McKellar (2), Nash Hadjerol (2), Zairene Lenizo (1). Jefferis Lab: Irene Salgarella (3). Scott Lab: Amanda Abusaif (11). Kim Lab: hanetwo (14),Chan Hyuk Kang (2).
55	SMP & SEZ: ADM09	720575940628462927	48		Anderson Lab: Altyn Rymbek (2). Jefferis Lab: Imaan Tamimi (6), Laia Serratosa (10), Rashmita Rana (1), Sangeeta Sisodiya (1). Murthy and Seung Labs: James Hebditch (1), Joshua Bañez (1), Mendell Lopez (58), Zairene Lenizo (2), J. Dolorosa (1). Kim Lab: Minsik Yun (1).

56	SMP & SEZ: pCd1?	720575940618057095	22		Jefferis Lab: A. Javier (1), Irene Salgarella (1). Murthy and Seung Labs: Austin T Burke (23)
57	SMP & SEZ: pCd1?	720575940604332460	12		Seung Lab: Zhihao Zheng (1). Jefferis and Wilson Labs: Laia Serratosa Capdevila (1). Jefferis: A. Javier (1), Bhargavi Parmar (1). Murthy and Seung Labs: Austin T Burke (13).
58	SMP & SEZ: ADM09p	720575940642910152	12		Scott Lab: Zepeng Yao (6). Murthy and Seung Labs: Austin T Burke (3), Shaina Mae Monungolh (1). Jefferis Lab: Yijie Yin (4), Marina Gkantia (10).
59	SMP & SEZ: DM3	720575940626005330	11		Janelia tracers: Tansy Yang (5). Jefferis Lab: Yijie Yin (3). Murthy and Seung Labs: Austin T Burke (7).
60	SMP & SEZ: Dh44	720575940618579505	10		Jefferis Lab: Imaan Tamimi (1), A. Javier (4), Rashmita Rana (1). Murthy and Seung Labs: Austin T Burke (13), remer tancontian (7).
61	SMP & SEZ: pCd1?	720575940645882420	10		Jefferis and Waddell Labs: Joseph Hsu (1). Murthy and Seung Labs: Austin T Burke (18), Joshua Bañez (1).
62	SMP & SEZ: pCd1?	720575940638671219	10		Jefferis Lab: A. Javier (3), Irene Salgarella (2), Tomke S (2), Varun Sane (5). Murthy and Seung Labs: Claire McKellar (2), remer tancontian (5), Nash Hadjerol (7).
63	SMP & SEZ: pCd1?	720575940622119861	8		Jefferis Lab: Irene Salgarella (2), Varun Sane (5), Yijie Yin (2). Murthy and Seung Labs: Austin T Burke (21).
64	SMP & SEZ: DM2_dorsal	720575940629754588	8		Anderson Lab: Altyn Rymbek (1). Jefferis Lab: Yijie Yin (11), Varun Sane (4). Murthy and Seung Labs: Austin T Burke (1), Joshua Bañez (1).
65	SMP & SEZ: SMPpv2	720575940621362044	7		Jefferis and Wilson Labs: Laia Serratosa Capdevila (1). Jefferis Lab: Yijie Yin (34), Irene Salgarella (1), Imaan Tamimi (7), Chitra Nair (1). Murthy and Seung Labs: Shirleyjoy Serona (1), Austin T Burke (1).
66	SMP & SEZ: FLA_R.NO_OUT.6	720575940623184567	7		Jefferis Lab: Katharina Eichler (1), Philipp Schlegel (1). Murthy and Seung Labs: Austin T Burke (1), Ben Silverman (2).
67	SMP & SEZ: pCd1?	720575940638719907	7		Jefferis and Waddell Labs: Joseph Hsu (1). Murthy and Seung Labs: Austin T Burke (1), Kyle Patrick Willie (6). Wes Murfin (29).
68	SMP & SEZ: pCd1?	720575940612572054	6		Seung Lab: Zhihao Zheng (1). Jefferis Lab: Irene Salgarella (6). Murthy and Seung Labs: Austin T Burke (37).
69	SMP & SEZ: DM2	720575940608174894	5		Anderson Lab: Altyn Rymbek (1), Jefferis and Waddell Labs: Joseph Hsu (14).
70	SMP & SEZ: DM2	720575940635196334	5		Jefferis Lab: Irene Salgarella (6). Janelia tracers: Tansy Yang (11). Murthy and Seung Labs: Austin T Burke (7).
71	SMP & SEZ: pMP5/DM2	720575940628732610	5		Murthy and Seung Labs: Austin T Burke (4), remer tancontian (5). Jefferis Lab: Irene Salgarella (3), Yijie Yin (22). Janelia tracers: Tansy Yang (2).
72	SMP & SEZ: SMP_R.FLA_L.29	720575940636113264	5		Jefferis Lab: Greg Jefferis (1), Laia Serratosa (11), Anjali Pandey (1). Dickson Lab: Alisa Poh (1). Murthy and Seung Labs: Nash Hadjerol (11).
73	SMP & SEZ: pCd1?	720575940638285184	5	203	Murthy and Seung Labs: Austin T Burke (3). Wes Murfin (9). Jefferis Lab: Laia Serratosa (4), Varun Sane (4).
74	Antler L	720575940622998967	54		Murthy and Seung Labs: Austin T Burke (17), Zairene Lenizo (4), Darrel Jay Akiatan (1), Shirleyjoy Serona (12), Shaina Mae Monungolh (2). Jefferis Lab: Yijie Yin (3).
75	Antler R	720575940631226439	50	104	Murthy and Seung Labs: Austin T Burke (17), Rey Adrian Candilada (3). Jefferis Lab: Varun Sane (7), Yijie Yin (5).
76	visual projection: SMP_R.SMP_R.201	720575940616608837	23		Jefferis Lab: Irene Salgarella (1), Rashmita Rana (1), Griffin Badalemente (4). Murthy and Seung Labs: J. Anthony Ocho (12), J. Dolorosa (1).
77	visual projection: SMP_R.SMP_R.698	720575940630512711	17		Jefferis Lab: Arti Yadav (1). Murthy and Seung Labs: Doug Bland (19).
78	visual projection: SMP_L.SMP_L.880	720575940636320063	15		Murthy and Seung Labs: J. Dolorosa (26). Jefferis Lab: Rashmita Rana (1).
79	visual projection: SMP_L.SMP_L.362	720575940620022960	12	67	Kim Lab: Dustin Garner (2). Jefferis Lab: Yijie Yin (16). Murthy and Seung Labs: Ben Silverman (5), remer tancontian (1).
80	Fan shaped body: DL1_dorsal; left	720575940626612254	29		Jefferis Lab: Rashmita Rana (1), Zeba Vohra (1). Murthy and Seung Labs: Austin T Burke (3), Kyle Patrick Willie (1).
81	Fan shaped body: FBl1-2	720575940642476448	17		Murthy and Seung Labs: Jay Gager (1), James Hebditch (4), Kendrick Joules Vinson (1). Jefferis Lab: Varun Sane (6), Yijie Yin (3).

82	Fan shaped body: FB.FB.473	720575940619615936	7		Jefferis Lab: Imaan Tamimi (1), A. Javier (1), Laia Serratosa (3), Arti Yadav (1), Sangeeta Sisodiya (7).
83	Fan shaped body: DL1	720575940613052200	5	58	Jefferis Lab: Varun Sane (3), Griffin Badalemente (1). Murthy and Seung Labs: Shaina Mae Monungolh (1).
84	Gallinule	720575940617054621	21		Jefferis Lab: Anjali Pandey (1). Murthy and Seung Labs: Mendell Lopez (1), Joshua Bañez (2).
85	Gallinule	720575940630349905	18		Seeds Hampel Lab: Lucia Kmecova (1). Huetteroth Lab: Wolf Huetteroth (3). Jefferis Lab: Laia Serratosa (3).
86	Gallinule	720575940629913130	7		Murthy and Seung Labs: Zairene Lenizo (12).
87	Gallinule	720575940620228449	5		Jefferis Lab: Yijie Yin (1). Murthy and Seung Labs: remer tancontian (10), Zairene Lenizo (1). Itisha Joshi (4).
88	Gallinule	720575940633711028	5	56	Murthy and Seung Labs: Claire McKellar (6)
89	SEZ: PRW.PRW.213	720575940625172016	16		Jefferis and Waddell Labs: Joseph Hsu (14). Murthy and Seung Labs: Darrel Jay Akiatan (31), Doug Bland (23), Austin T Burke (1), Ryan Willie (3), remer tancontian (1).
90	SEZ: PRW.GNG.43	720575940630664556	8		Jefferis Lab: Marta Costa (1), Sangeeta Sisodiya (2). Seeds Hampel Lab: Alexis E Santana Cruz (2). Murthy and Seung Labs: Zairene Lenizo (3), Darrel Jay Akiatan (5), Ariel Dagohoy (1), Rey Adrian Candilada (2), Joshua Bañez (1), Nash Hadjerol (6), remer tancontian (1).
91	SEZ: PRW.PRW.312	720575940632055521	7		Murthy and Seung Labs: J. Dolorosa (3), Shirleyjoy Serona (103). Jefferis Lab: Arti Yadav (1).
92	SEZ: PRW.PRW.82	720575940616860758	6		Jefferis Lab: Arti Yadav (1). Murthy and Seung Labs: Joshua Bañez (7), Zairene Lenizo (3), Doug Bland (12), J. Dolorosa (2), remer tancontian (1).
93	SEZ: PRW.PRW.164	720575940622457579	6	43	Jefferis Lab: Arti Yadav (1). Murthy and Seung Labs: Michelle Pantujan (2), Shirleyjoy Serona (3).
				1742	

Table S3: CCAP presynaptic partners

Name	Flywire ID	synapses from BiT2 (720575940621662332)	synapses from VESa1 (720575940632951597)	synapses from CCHa2R-RA (720575940621942021)	synapses from CCHa2R-RA (720575940627765903)	synapses from Cowboy (720575940611730674)	Total synapses	Tracing contributions (number of edits)
CCAP	720575940646160948	18	8	9	5	0	40	Jefferis Lab: Greg Jefferis (15), Zeba Vohra (17), A. Javier (14), Siqi Fang (9), Varun Sane (6), Dhara Kakadiya (4). Jefferis and Wilson: Laia Serratosa Capdevila (1). Murthy and Seung Labs: Michelle Pantujan (1), Shaina Mae Monungolh (1), Rey Adrian Candilada (2), regine salem (1), Nash Hadjerol (1), Joshua Bañez (1).

CCAP	7205759 4062114 8993	19	14	5	7	5	50	Murthy and Seung Labs: Austin T Burke (5), Rey Adrian Candilada (1), J. Anthony Ocho (8), Nash Hadjerol (26), Joshua Bañez (4), Ryan Willie (2). Jefferis Lab: A. Javier (28), Imaan Tamimi (1), Katharina Eichler (11), Mendell Lopez (80). Jefferis and Wilson Labs: Laia Serratosa Capdevila (2), Varun Sane (1). Janelia tracers: Tansy Yang (1).
Total synapses per cell type		37	22	14	12	5	90	

940

941

942

943

944

945

946

947

948

949

950

951

952

953

954

955

Table S4: Fly genotypes in figures

Figure	Short Genotype	Full Genotype
1A	nSyb	w1118 ; UAS-dcr2/+ ; UAS-nSynaptobrevin RNAi (attP2)/+
1A	nSyb	w1118 ; UAS-dcr2/+; UAS-nSynaptobrevin (attP2)/VT011155-Gal4 (attP2)
1A	TRH	w1118 ; UAS-dcr2/+ ; UAS-Trh RNAi (attP2)/+
1A	TRH	w1118 ; UAS-dcr2/+ ; UAS-Trh RNAi (attP2)/VT011155-Gal4 (attP2)
1A	ChAT	w1118 ; UAS-dcr2/+ ; UAS- ChAT RNAi (attP2)/+

1A	ChAT	w1118 ; UAS-dcr2/+ ; UAS- ChAT RNAi (attP2)/VT011155-Gal4 (attP2)
1A	TBH	w1118 ; UAS-dcr2/+ ; UAS-Tbh RNAi (attP2)/+
1A	TBH	w1118 ; UAS-dcr2/+ ; UAS-Tbh RNAi (attP2)/VT011155-Gal4 (attP2)
1A	HDC	w1118 ; UAS-dcr2/+ ; UAS-Hdc RNAi (attP2)/+
1A	HDC	w1118 ; UAS-dcr2/+ ; UAS-Hdc RNAi (attP2)/VT011155-Gal4 (attP2)
1A	VMAT	w1118 ; UAS-dcr2/+; UAS-VMAT RNAi (attP2)/+
1A	VMAT	w1118 ; UAS-dcr2/+ ; UAS-VMAT RNAi (attP2)/VT011155-Gal4 (attP2)
1A	GAD1	w1118 ; UAS-dcr2/+; UAS-GAD1 RNAi (attP2)/+
1A	GAD1	w1118 ; UAS-dcr2/+ ; UAS-GAD1 RNAi (attP2)/VT011155-Gal4 (attP2)
1A	DDC	w1118 ; UAS-dcr2/+ ; UAS-DDC RNAi (attP2)/+
1A	DDC	w1118 ; UAS-dcr2/+ ; UAS-DDC RNAi (attP2)/VT011155-Gal4 (attP2)
1A	DVGlut	w1118 ; UAS-dcr2/+ ; UAS-DVGlut RNAi (attP2)/+
1A	DVGlut	w1118 ; UAS-dcr2/+ ; UAS-DVGlut RNAi (attP2)/VT011155-Gal4 (attP2)
1A	sNPF	w1118 ; UAS-dcr2/+ ; UAS-sNPF RNAi (attP2)/+
1A	sNPF	w1118 ; UAS-dcr2/+ ; UAS-sNPF RNAi (attP2)/VT011155-Gal4 (attP2)
1A	VGAT	w1118 ; UAS-dcr2/+ ; UAS-VGAT RNAi (attP2)/+
1A	VGAT	w1118 ; UAS-dcr2/+ ; UAS-VGAT RNAi (attP2)/VT011155-Gal4 (attP2)
1A	TDC2	w1118 ; UAS-dcr2/+ ; UAS-Tdc2 RNAi (attP2)/+
1A	TDC2	w1118 ; UAS-dcr2/+ ; UAS-Tdc2 RNAi (attP2)/VT011155-Gal4 (attP2)
1A	dILP1	w1118 ; UAS-dcr2/+ ; UAS-dILP1 RNAi (attP2)/+
1A	dILP1	w1118 ; UAS-dcr2/+ ; UAS-dILP1 RNAi (attP2)/VT011155-Gal4 (attP2)
1A	dILP2	w1118 ; UAS-dcr2/+ ; UAS-dILP2 RNAi (attP2)/+
1A	dILP2	w1118 ; UAS-dcr2/+ ; UAS-dILP2 RNAi (attP2)/VT011155-Gal4 (attP2)
1A	dILP3	w1118 ; UAS-dcr2/+ ; UAS-dILP3 RNAi (attP2)/+
1A	dILP3	w1118 ; UAS-dcr2/+ ; UAS-dILP3 RNAi (attP2)/VT011155-Gal4 (attP2)
1A	dILP4	w1118 ; UAS-dcr2/+ ; UAS-dILP4 RNAi (attP2)/+
1A	dILP4	w1118 ; UAS-dcr2/+ ; UAS-dILP4 RNAi (attP2)/VT011155-Gal4 (attP2)
1A	dILP5	w1118 ; UAS-dcr2/+ ; UAS-dILP5 RNAi (attP2)/+
1A	dILP5	w1118 ; UAS-dcr2/+ ; UAS-dILP5 RNAi (attP2)/VT011155-Gal4 (attP2)
1A	dILP6	w1118 ; UAS-dcr2/+ ; UAS-dILP6 RNAi (attP2)/+
1A	dILP6	w1118 ; UAS-dcr2/+ ; UAS-dILP6 RNAi (attP2)/VT011155-Gal4 (attP2)
1A	dILP7	w1118 ; UAS-dcr2/+ ; UAS-dILP7 RNAi (attP2)/+

1A	dILP7	w1118 ; UAS-dcr2/+ ; UAS-dILP7 RNAi (attP2)/VT011155-Gal4 (attP2)
1B	dILP3 RNAi	w1118 ; + ; UAS-dILP3 RNAi (attP2)/+
1B	dILP3 RNAi	w1118 ; + ; UAS-dILP3 RNAi (attP2)/VT011155-Gal4 (attP2)
1B	Amon RNAi	w1118/w* ; + ; UAS-amon RNAi (attP2)/+
1B	Amon RNAi	w1118/w* ; + ; UAS-amon RNAi (attP2)/VT011155-Gal4 (attP2)
1B	ISN-Gal4	w1118 ; + ; VT011155-Gal4 (attP2)/+
1D	ISN-Gal4 > tdT	w1118/w* ; UAS-myrGFP.QUAS-mtdTomato-3xHA/+; trans-Tango/VT011155-Gal4 (attP2)
2B,2F	BiT split-Gal4 > Chrimson	w1118, UAS-IVS-CsChrimson.mVenus (attP18)/+; VT002073-Gal4.AD (attP40)/+; VT040568-Gal4.DBD (attP2)/+
2D, 2E	ISN > Chrimson, BiT > ArcLight	13XLexAop2-IVS-p10-ChrimsonR-mCherry (attP18)/w1118; GMR34G02-LexA (attP40)/VT002073-Gal4.AD (attP40); VT040568-Gal4.DBD (attP2)/UAS-ArcLight (attP2)
2F, 2G	BiT split-Gal4	w1118; VT002073-Gal4.AD (attP40)/+; VT040568-Gal4.DBD (attP2)/+
2F	Empty split-Gal4 > Chrimson	w1118, UAS-IVS-CsChrimson.mVenus (attP18); p65-AD.empty (attp40)/+; GAL4-DBD.empty (attP2)/+
2F	Gr5a-Gal4 > Chrimson	w1118, UAS-IVS-CsChrimson.mVenus (attP18); Gr5a-Gal4/+; Gr5a-Gal4/+
2F	ppk28-Gal4 > Chrimson	w1118, UAS-IVS-CsChrimson.mVenus (attP18); + ; ppk28-Gal4/+
2G	BiT split-Gal4 > nSyb RNAi	w1118; VT002073-Gal4.AD (attP40)/+; VT040568-Gal4.DBD (attP2)/UAS-nSynaptobrevin RNAi (attP2)
2G, 4G, 5G	nSyb RNAi	w1118; +; UAS-nSynaptobrevin RNAi (attP2)/+
4B, 4F	CCHa2R (RA) > Chrimson	w1118, UAS-IVS-CsChrimson.mVenus (attP18)/w1118; TI{2A-GAL4}CCHa2-R[2A-A.GAL4]/+; +
4D, 4E	ISN > Chrimson, CCHa2R (RA) > GCaMP	w1118; GMR34G02-LexA (attP40)/ TI{2A-GAL4}CCHa2-R[2A-A.GAL4]; LexAop-Chrimson,UAS-GCaMP6s/TM2
4F, 4G	CCHa2R (RA)	w1118; TI{2A-GAL4}CCHa2-R[2A-A.GAL4]/+; +
4F, 5F	UAS-Chrimson	w1118, UAS-IVS-CsChrimson.mVenus (attP18)/w1118; +; +
4G	CCHa2R (RA) > nSyb RNAi	w1118; TI{2A-GAL4}CCHa2-R[2A-A.GAL4]/+; UAS-nSynaptobrevin RNAi (attP2)/+
5B, 5F	CCAP > Chrimson	w1118, UAS-IVS-CsChrimson.mVenus (attP18)/w1118; CCAP-Gal4/+; +
5D, 5E	ISN > Chrimson, CCAP > GCaMP	w1118, 13XLexAop2-IVS-p10-ChrimsonR-mCherry (attP18)/w1118; GMR34G02-LexA (attP40)/CCAP-Gal4; 20XUAS-IVS-jGCaMP7b(VK00005)/+
5F, 5G	CCAP	w1118; CCAP-Gal4/+; +
5G	CCAP > NSyb RNAi	w1118; CCAP-Gal4/+; UAS-nSynaptobrevin RNAi (attP2)/+
Supp 1A	ISN > transTango	w*/w1118 ; UAS-myrGFP.QUAS-mtdTomato-3xHA/+; trans-Tango/VT011155-Gal4 (attP2)

Supp 2A,B	BiT genetic control	w1118, 13XLexAop2-IVS-p10-ChrimsonR-mCherry (attP18)/w1118; VT002073-Gal4.AD (attP40)/+; VT040568-Gal4.DBD (attP2)/UAS-ArcLight (attP2)
Supp 3A,B	BiT > Chrimson, IPC > GCaMP	10XUAS-syn21-Chrimson88-tdT3.1 (attP18), LexAop2-syn21-opGCaMP6s suHw (attP8)/w1118; TI{2A-lexA::GAD}CCHa2-R[2A-A.lexA]/VT002073-Gal4.AD (attP40); VT040568-Gal4.DBD (attP2)/+
Supp 3C,D	IPC genetic control	10XUAS-syn21-Chrimson88-tdT3.1 (attP18), LexAop2-syn21-opGCaMP6s suHw (attP8)/w1118; dILP2-LexA/CyO; TM2/TM3, Sb
Supp 4A,B	CCHa2R (RA) genetic control	w1118; TI{2A-GAL4}CCHa2-R[2A-A.GAL4]/CyO; LexAop-Chrimson,UAS-GCaMP6s/TM2
Supp 4C,D	BiT > Chrimson, CCHa2R (RA) > GCaMP	10XUAS-syn21-Chrimson88-tdT3.1 (attP18), LexAop2-syn21-opGCaMP6s suHw (attP8)/w1118; TI{2A-lexA::GAD}CCHa2-R[2A-A.lexA]/VT002073-Gal4.AD (attP40); VT040568-Gal4.DBD (attP2)/+
Supp 5	ISN > Chrimson, CCAP > GCaMP	13XLexAop2-IVS-p10-ChrimsonR-mCherry (attP18)/w1118; GMR34G02-LexA (attP40)/+ ; 20XUAS-IVS-jGCaMP7b(VK00005)/CCAP-Gal4

956

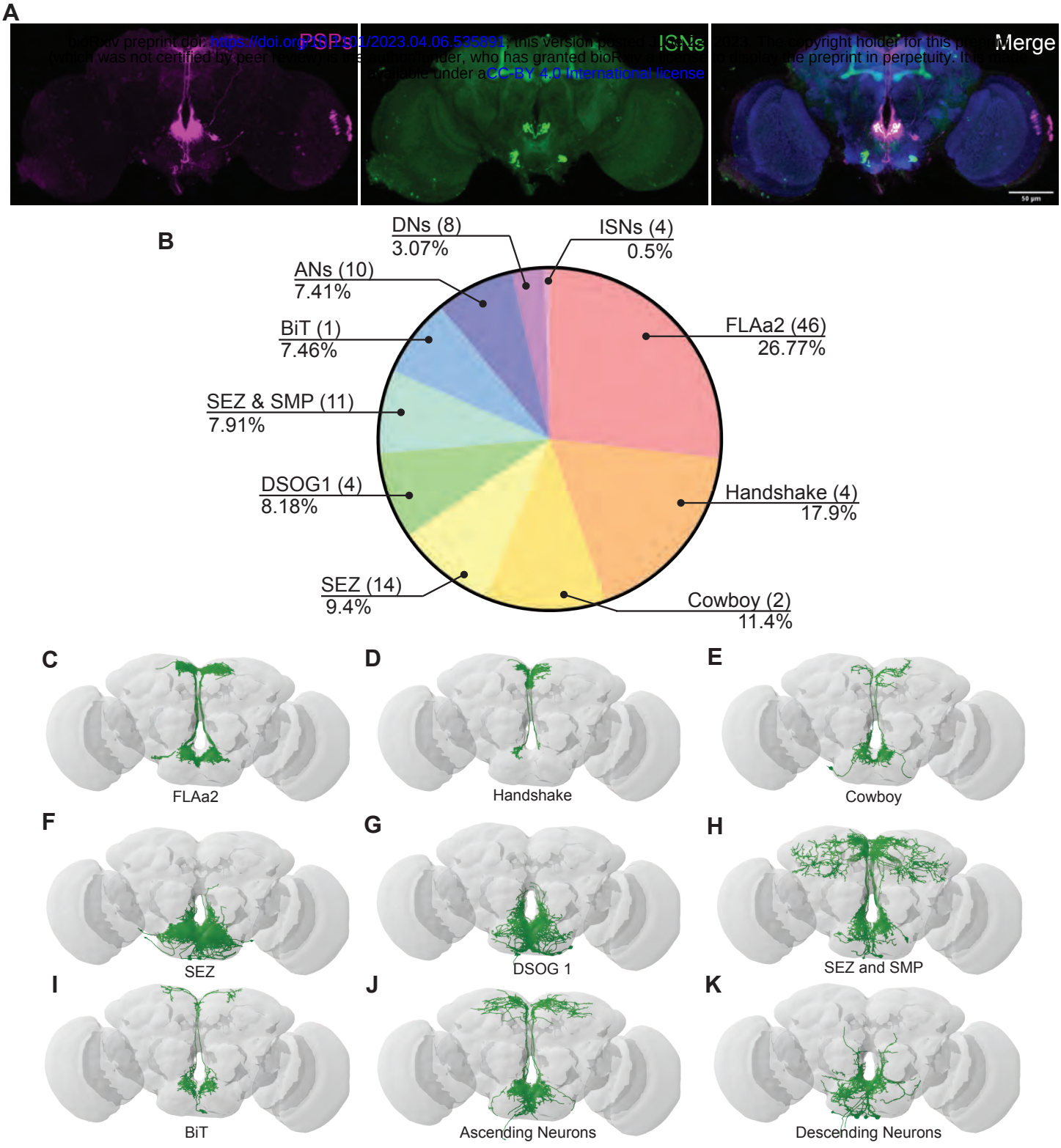

Figure 1 - supplement 1. ISN postsynaptic partners labeled by trans-Tango and EM
(A) Expression of trans-Tango ligand in the ISNs (green) and postsynaptic partners (PSPs) (magenta). nc82 staining in blue. (B) Distribution of synaptic output from the ISNs divided by cell class or brain region. Total of 4050 synapses from the ISNs and 104 postsynaptic partners. FLAa2 (46 neurons) receive 26.77% of all ISN output, Handshake (4 neurons) 17.9%, Cowboy (2 neurons) 11.4%, neurons located in the subesophageal zone (SEZ) (14 neurons) 9.04%, DSOG1 (4 neurons) 8.18%, neurons with neurites in the subesophageal zone and superior medial protocerebrum (SEZ & SMP) (11 neurons) 7.91%, BiT (1 neuron) 7.46%, Ascending neurons (ANs) (10 neurons) 4.41%, Descending neurons (DNs) (8 neurons) 3.07%, and ISNs (4 neurons) 0.5%. Only postsynaptic partners with 5 or more synapses were considered for this analysis. Reconstruction of FLAa2 neurons (C), Handshake neurons (D), Cowboy neurons (E), neurons innervating the SEZ (F), DSOG1 neurons (G), neurons innervating the SEZ & SMP (H), BiT (I), ascending neurons (J), descending neurons (K).

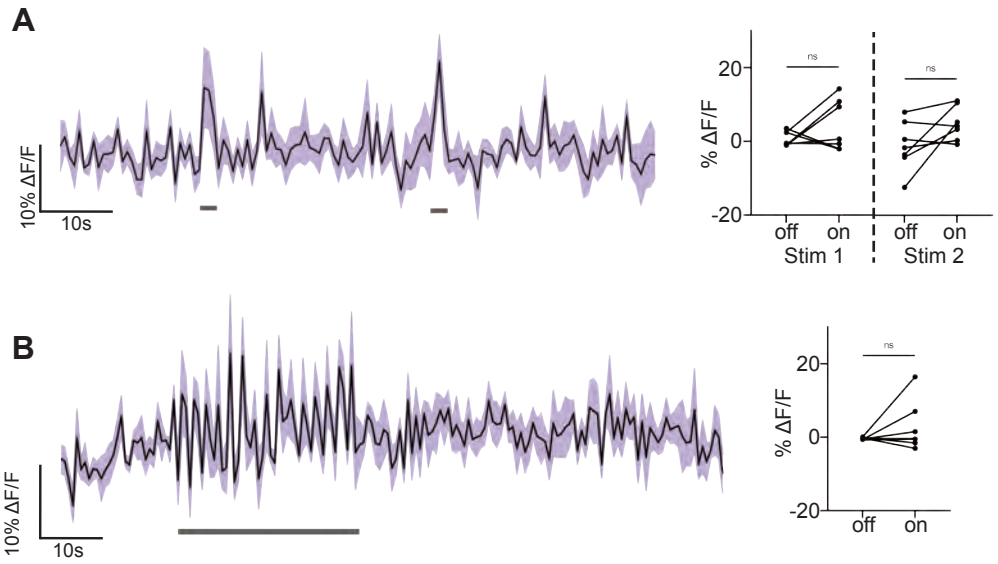

Figure 2 - supplement 2. BiT genetic control functional imaging
Genetic controls: we expressed the light sensitive ion channel Chrimson without the ISN-LexA driver and exposed the brains to 660nm LED. We expressed the voltage sensor ArcLight in BiT and imaged it with a 2 photon microscope. (A) ArcLight response of BiT soma to 2s LED exposure or (B) 30s LED exposure. Left: Scatter plot shows mean +/- SEM of all flies imaged, gray bars represent LED stimulation. Right: Quantification of mean fluorescence intensity before stim (off) and during stim (on), each dot represents one fly. Paired Wilcoxon or paired t-test. n=7 flies.

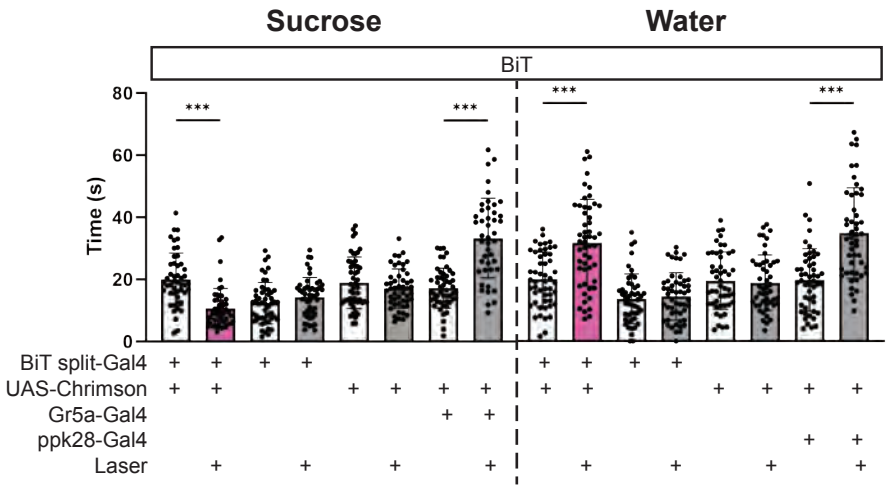

Figure 2 - supplement 2. BiT optogenetic activation ingestion phenotype

Temporal consumption assay for 1M sucrose or water during acute optogenetic activation of BiT with Chrimson. Represented are the mean, and the 10-90 percentile. Data was analyzed using Kruskal-Wallis test, followed by multiple comparisons against the no laser control. n=44-54 animals/genotype. ***p<0.001

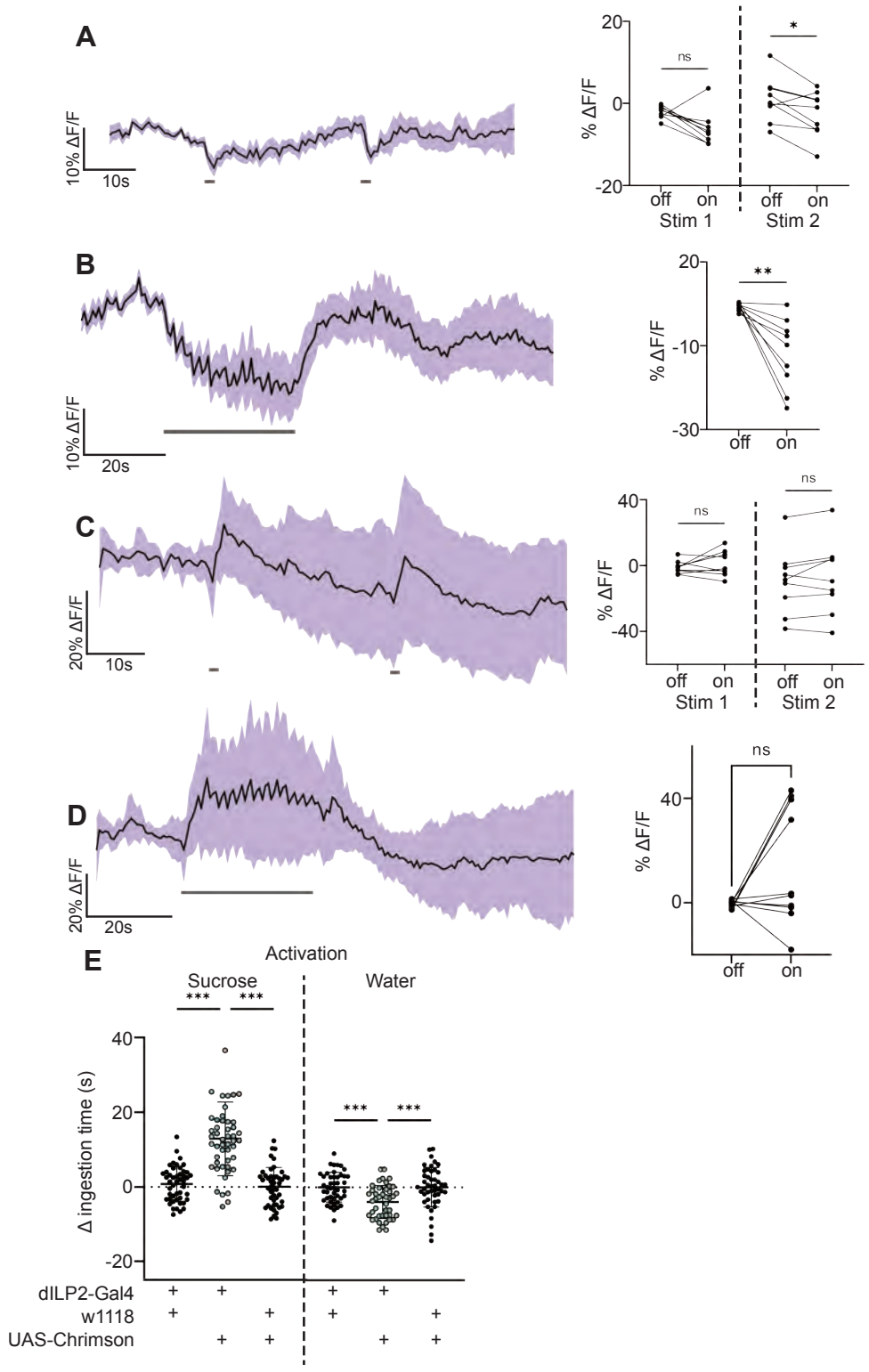

Figure 3 - supplement 1. IPC response to BiT stimulation

A and B: We expressed the light sensitive ion channel Chrimson in BiT and optogenetically stimulated it with 660nm LED. We expressed the calcium sensor GCaMP in the IPCs and imaged them with a 2 photon microscope. (A) Calcium response of IPC somas to 2s optogenetic activation of BiT or (B) 30s optogenetic activation of BiT. Left: Scatter plot shows mean +/- SEM of all flies imaged, gray bars represent LED stimulation. Right: Quantification of mean fluorescence intensity before stim (off) and during stim (on), each dot represents one fly. Paired Wilcoxon test or paired t-test. n=9 flies. C and D: Genetic controls: we expressed the light sensitive ion channel Chrimson without the BiT-split Gal4 driver and exposed the brains to 660nm LED. We expressed the calcium sensor GCaMP in the IPCs and imaged them with a 2 photon microscope. (C) Calcium response of IPC somas to 2s LED exposure or (D) 30s LED exposure. Left: Scatter plot shows mean +/- SEM of all flies imaged, gray bars represent LED stimulation. Right: Quantification of mean fluorescence intensity before stim (off) and during stim (on), each dot represents one fly. Paired t-test. n=9-10 flies. (E) Temporal consumption assay for 1M sucrose or water during acute optogenetic activation of IPCs with Chrimson. Ingestion time of females exposed to light normalized to dark controls of indicated genotype. One-way ANOVA with Holm-Šídák multiple comparison test. n=43-49 animals/genotype. *p<0.05, **p<0.01, ***p<0.001

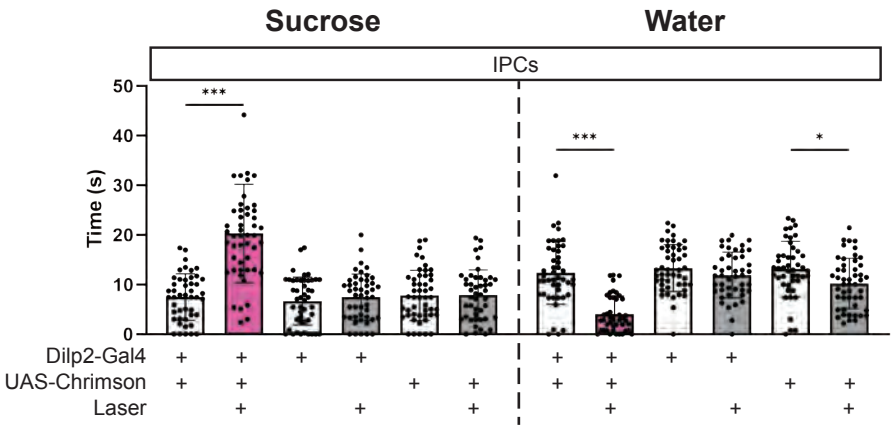

Figure 3 - supplement 2. IPC optogenetic activation ingestion phenotype

Temporal consumption assay for 1M sucrose or water during acute optogenetic activation of IPCs with Chrimson. Represented are the mean, and the 10-90 percentile. Data was analyzed using One-way ANOVA, followed by multiple comparisons against the no laser control. n=43-49 animals/genotype. *p<0.05, ***p<0.001

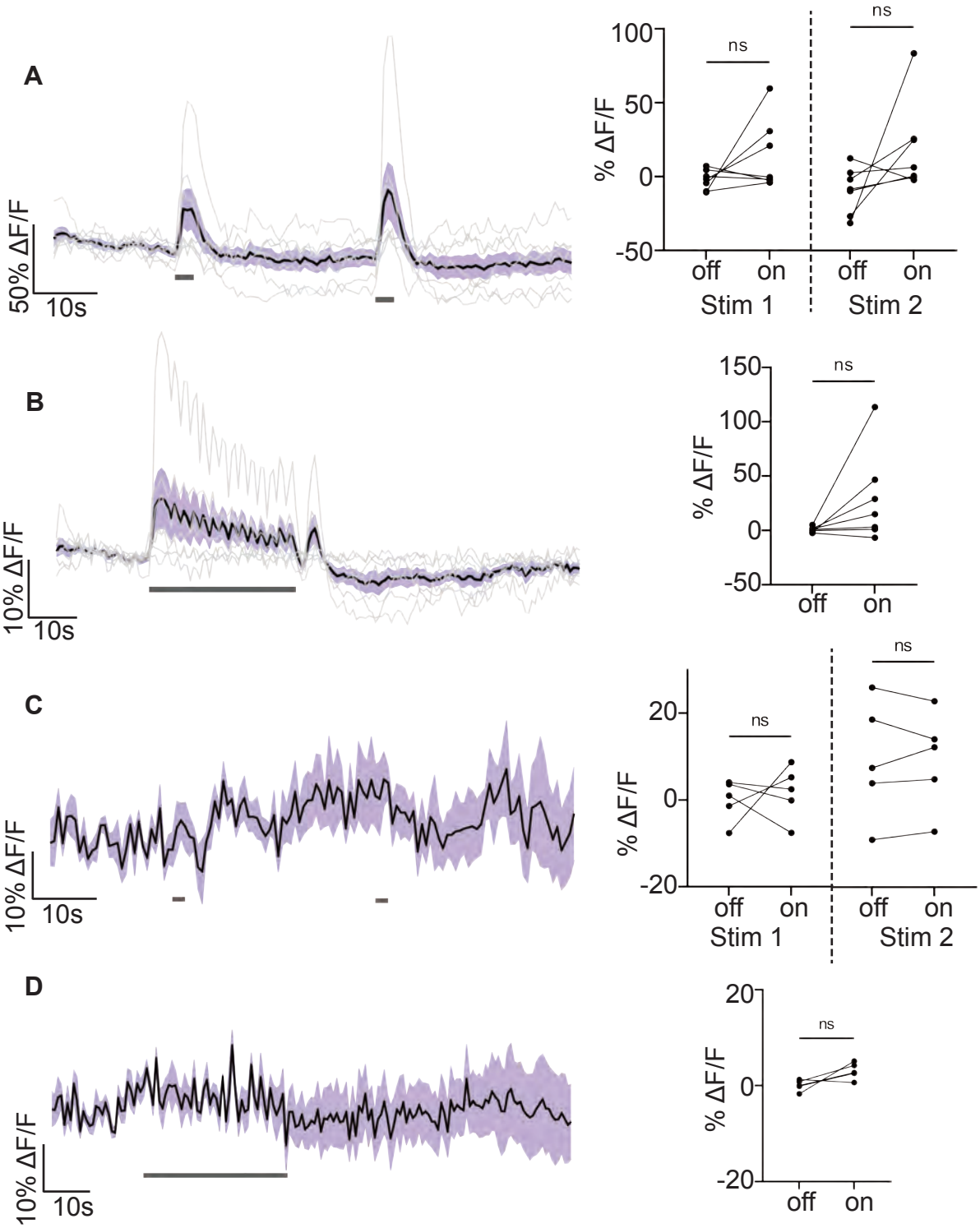

Figure 4 - supplement 1. CCHa2R-RA genetic controls functional imaging and response to BiT optogenetic stimulation

A and B: Genetic controls: we expressed the light sensitive ion channel Chrimson without the ISN-LexA driver and exposed the brains to 660nm LED. We expressed the calcium sensor GCaMP in the CCHa2R-RA neurons and imaged them with a 2 photon microscope. (A) Calcium response of CCHa2R-RA SEZ neurites to 2s LED exposure or (B) 30s LED exposure. Left: Scatter plot shows mean +/- SEM of all flies imaged, with individual traces in gray, gray bars represent LED stimulation. Right: Quantification of mean fluorescence intensity before stim (off) and during stim (on), each dot represents one fly. Paired Wilcoxon test and paired t-test. n=7 flies. C and D: We expressed the light sensitive ion channel Chrimson in BiT and optogenetically stimulated it with 660nm LED. We expressed the calcium sensor GCaMP in the CCHa2R-RA neurons and imaged them with a 2 photon microscope. (C) Calcium response of CCHa2R-RA somas to 2s optogenetic stimulation of BiT or (D) 30s optogenetic stimulation of BiT. Left: Scatter plot shows mean +/- SEM of all flies imaged, gray bars represent LED stimulation. Right: Quantification of mean fluorescence intensity before stim (off) and during stim (on), each dot represents one fly. Paired t-test. n=5 flies.

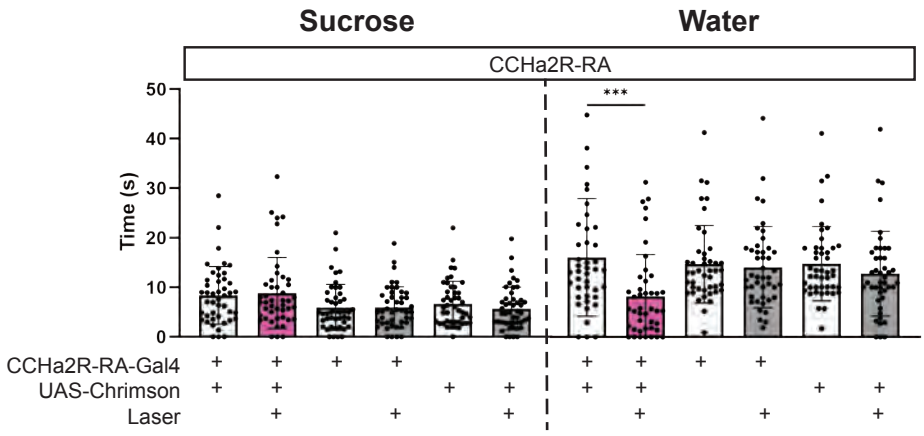

Figure 4 - supplement 2. CCHa2R-RA optogenetic activation ingestion phenotype
Temporal consumption assay for 1M sucrose or water during acute optogenetic activation of CCHa2R-RA neurons with Chrimson. Represented are the mean, and the 10-90 percentile. Data was analyzed using Kruskal-Wallis test, followed by multiple comparisons against the no laser control. n=42-47 animals/genotype. ***p<0.001

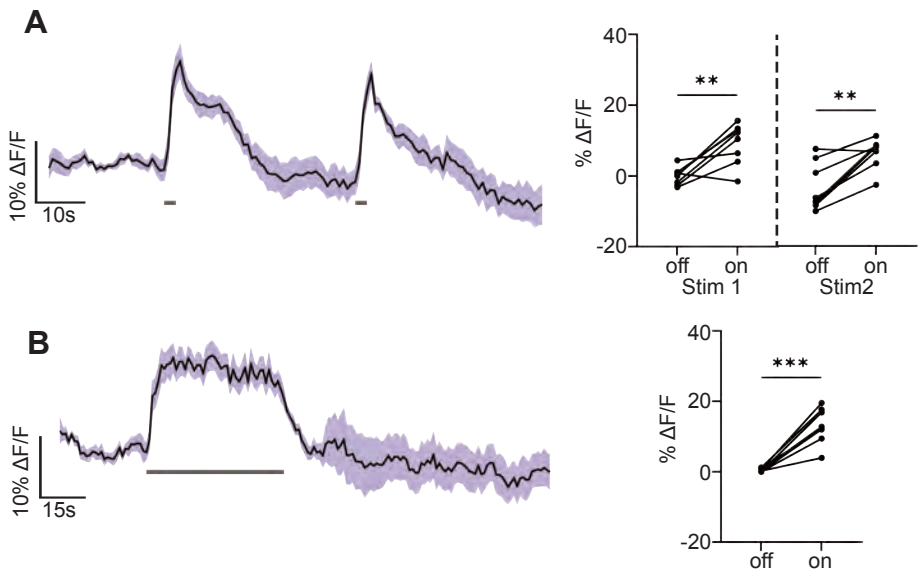

Figure 5 - supplement 1. CCAP response to ISN activation using another CCAP-Gal4 driver

We expressed the light sensitive ion channel Chrimson in the ISNs and optogenetically stimulated them with 660nm LED. We expressed the calcium sensor GCaMP in the CCAP neurons and imaged them with a 2 photon microscope. (A) Calcium response of CCAP neurites to 2s optogenetic stimulation of the ISNs or (B) 30s optogenetic stimulation of the ISNs. Left: Scatter plot shows mean +/- SEM of all flies imaged, gray bars represent LED stimulation. Right: Quantification of mean fluorescence intensity before stim (off) and during stim (on), each dot represents one fly. Paired t-test. n=8 flies. **p<0.01, ***p<0.001

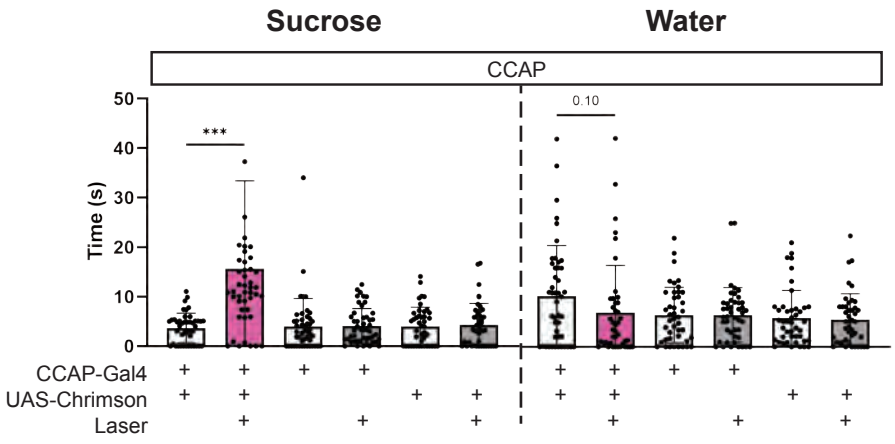

Figure 5 - supplement 2. CCAP optogenetic activation ingestion phenotype
Temporal consumption assay for 1M sucrose or water during acute optogenetic activation of CCAP neurons with Chrimson. Represented are the mean, and the 10-90 percentile. Data was analyzed using Kruskal-Wallis test, followed by multiple comparisons against the no laser control. n=42-48 animals/genotype. ***p<0.001